US 20020002992A1

(19) United States

(12) Patent Application Publication (10) Pub. No.: US 2002/0002992 A1

KARIYA et al. (43) Pub. Date: Jan. 10, 2002

(54) PHOTOVOLTAIC ELEMENT

(76) Inventors: TOSHIMITSU KARIYA, SORAKU-GUN (JP); MASAFUMI SANO, SORAKU-GUN (JP); YUTAKA NISHIO, KYOTANABE-SHI (JP)

Correspondence Address:
FITZPATRICK CELLA HARPER & SCINTO
30 ROCKEFELLER PLAZA
NEW YORK, NY 10112 (US)

(*) Notice: This is a publication of a continued prosecution application (CPA) filed under 37 CFR 1.53(d).

(21) Appl. No.: 09/340,464

(22) Filed: Jun. 28, 1999

(30) Foreign Application Priority Data

Jun. 30, 1998 (JP) 10-183884

Publication Classification

(51) Int. Cl.[7] H02N 6/00

(52) U.S. Cl. 136/255; 136/252; 136/256; 136/257; 257/432; 257/436

(57) ABSTRACT

Provided is a photovoltaic element comprising a p-type semiconductor layer and a transparent conductive layer comprised of indium tin oxide bonded to each other at a surface, wherein the sum of tin oxide content and tin content of the transparent conductive layer varies in the layer thickness direction and is minimum at the bonding surface of the p-type semiconductor layer and the transparent conductive layer. Thus provided is a photovoltaic element which has a high photoelectric conversion efficiency with less lowering even when exposed to an intense light for a long term.

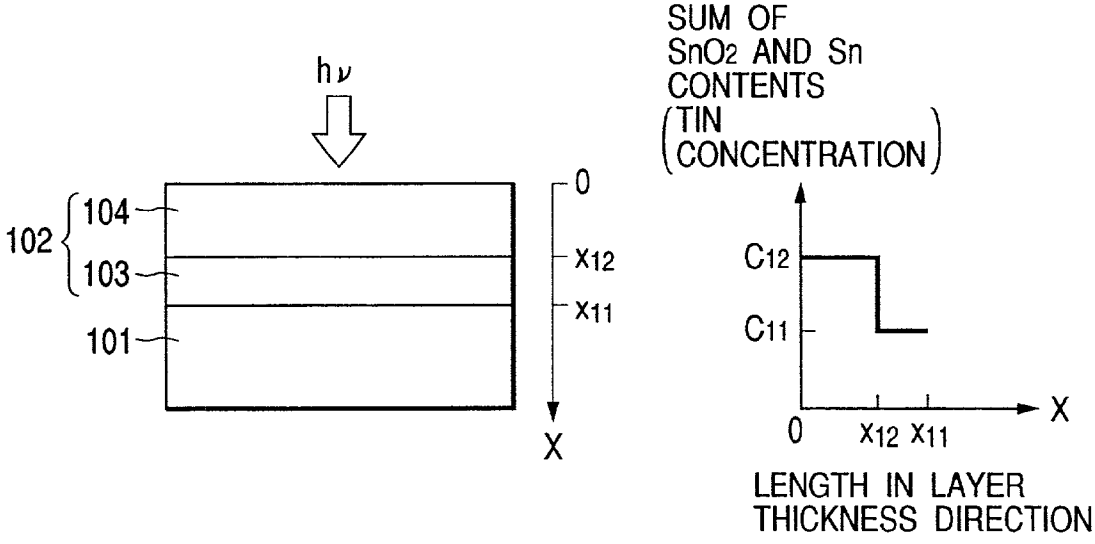

FIG. 1

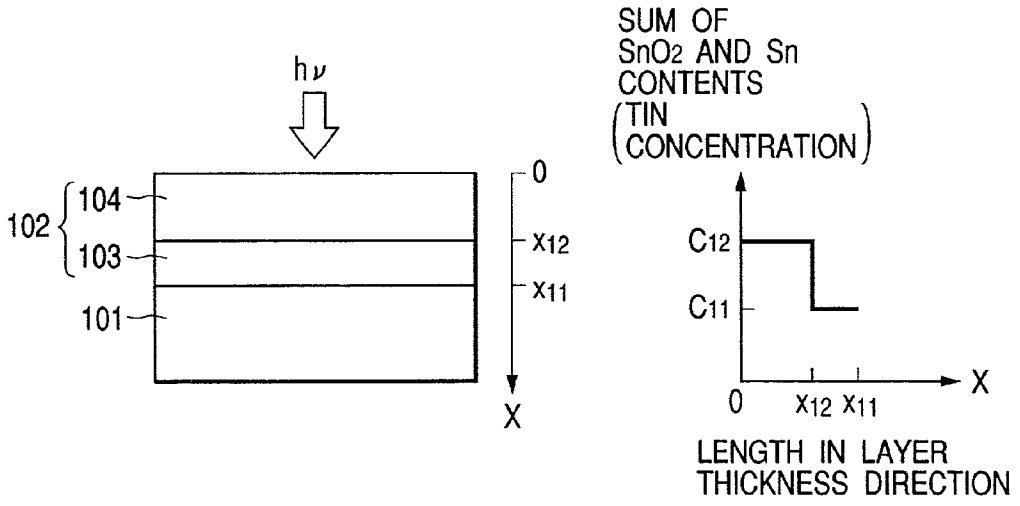
hν
102
104
103
101
0
X12
X11
X
SUM OF SnO2 AND Sn CONTENTS (TIN CONCENTRATION)
C12
C11
0
X12 X11
X
LENGTH IN LAYER THICKNESS DIRECTION

FIG. 2

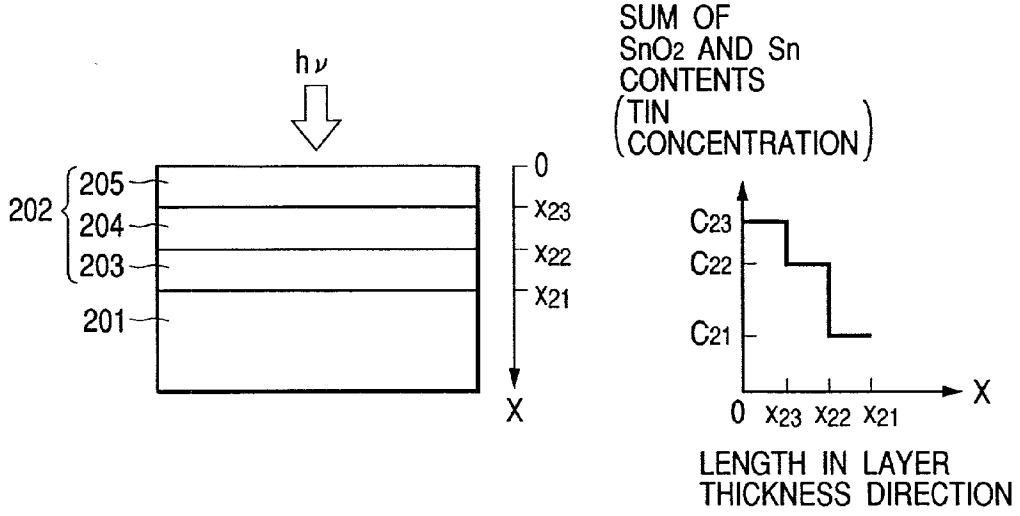
hν
202
205
204
203
201
0
X23
X22
X21
X
SUM OF SnO2 AND Sn CONTENTS (TIN CONCENTRATION)
C23
C22
C21
0
X23 X22 X21
X
LENGTH IN LAYER THICKNESS DIRECTION

FIG. 3 PRIOR ART

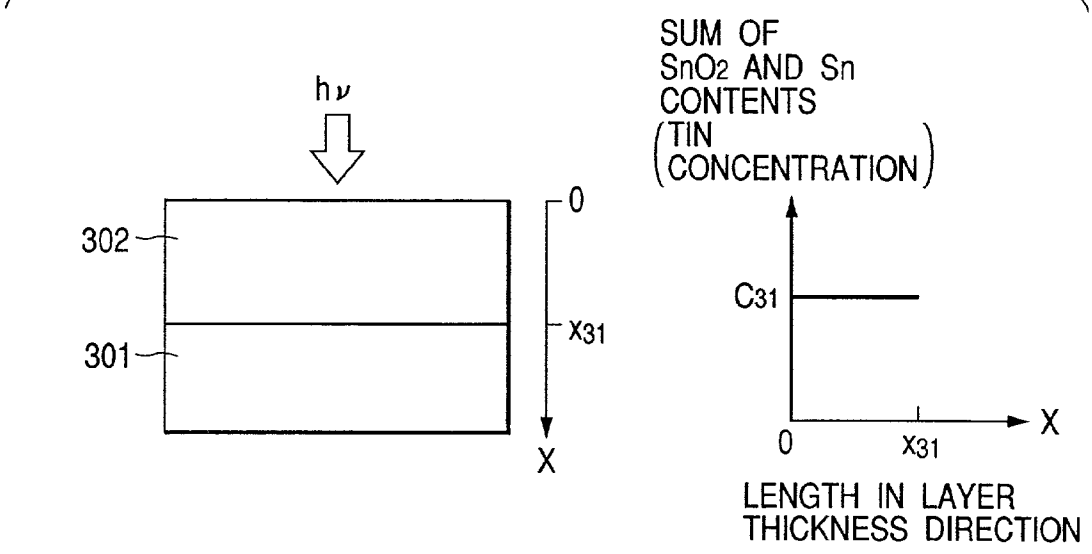

FIG. 4

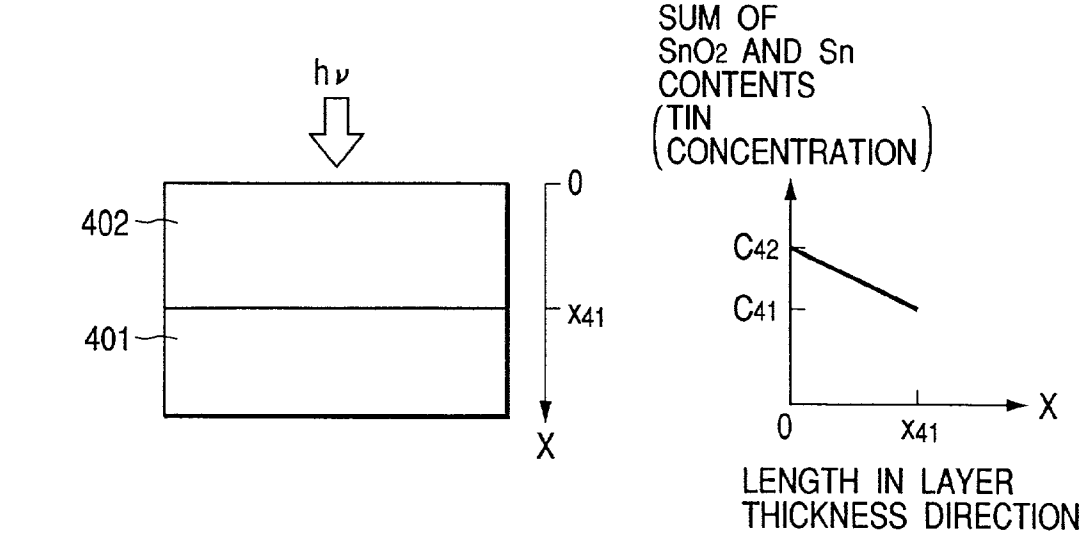

FIG. 5

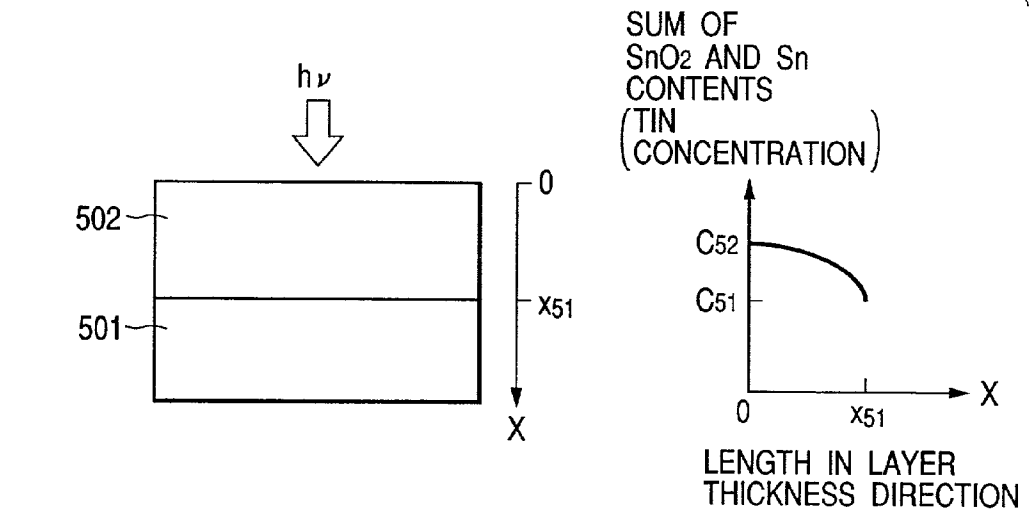
hν
502
501
0
x51
X
SUM OF SnO2 AND Sn CONTENTS (TIN CONCENTRATION)
C52
C51
0
x51
X
LENGTH IN LAYER THICKNESS DIRECTION

FIG. 6

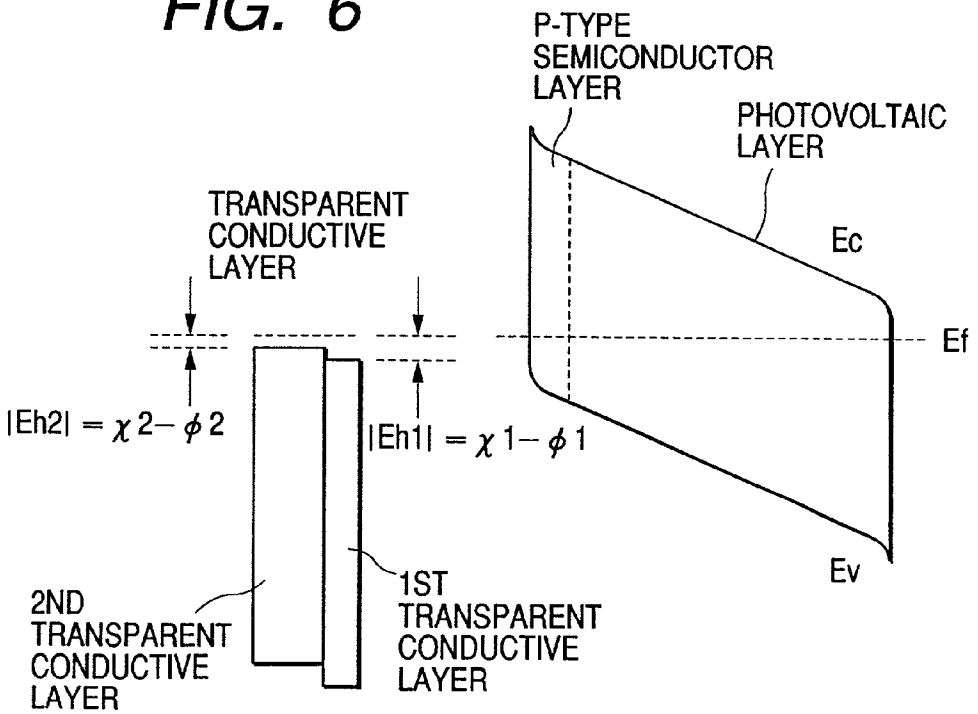
P-TYPE SEMICONDUCTOR LAYER
PHOTOVOLTAIC LAYER
TRANSPARENT CONDUCTIVE LAYER
Ec
Ef
Ev
|Eh2| = χ2 − φ2
|Eh1| = χ1 − φ1
2ND TRANSPARENT CONDUCTIVE LAYER
1ST TRANSPARENT CONDUCTIVE LAYER

FIG. 7

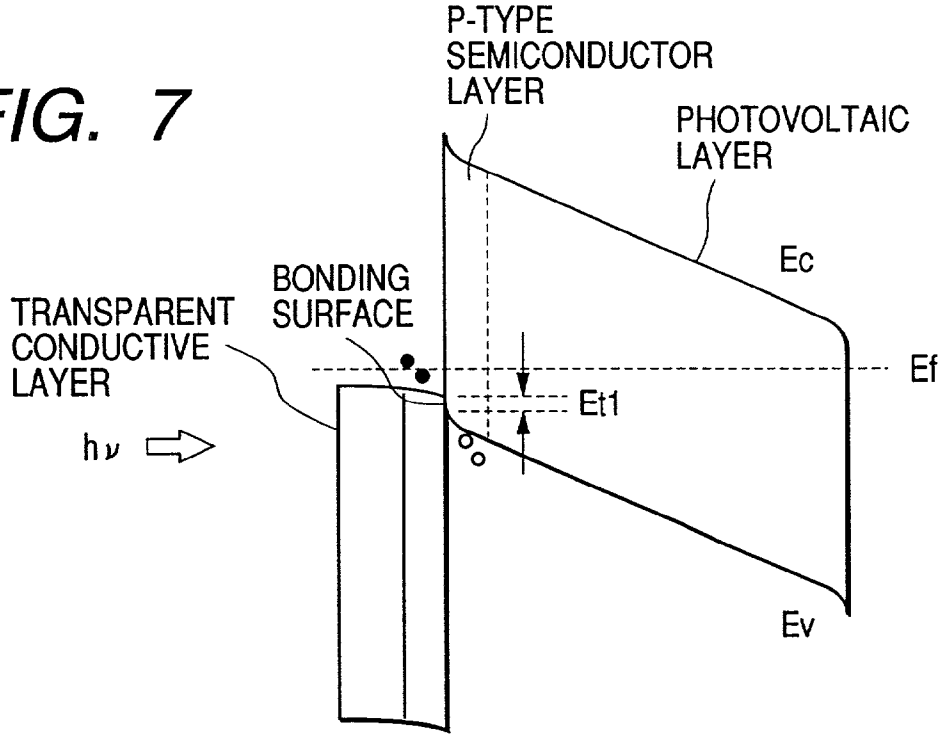
P-TYPE
SEMICONDUCTOR
LAYER
PHOTOVOLTAIC
LAYER
Ec
BONDING
SURFACE
TRANSPARENT
CONDUCTIVE
LAYER
Ef
Et1
hν
Ev

FIG. 8

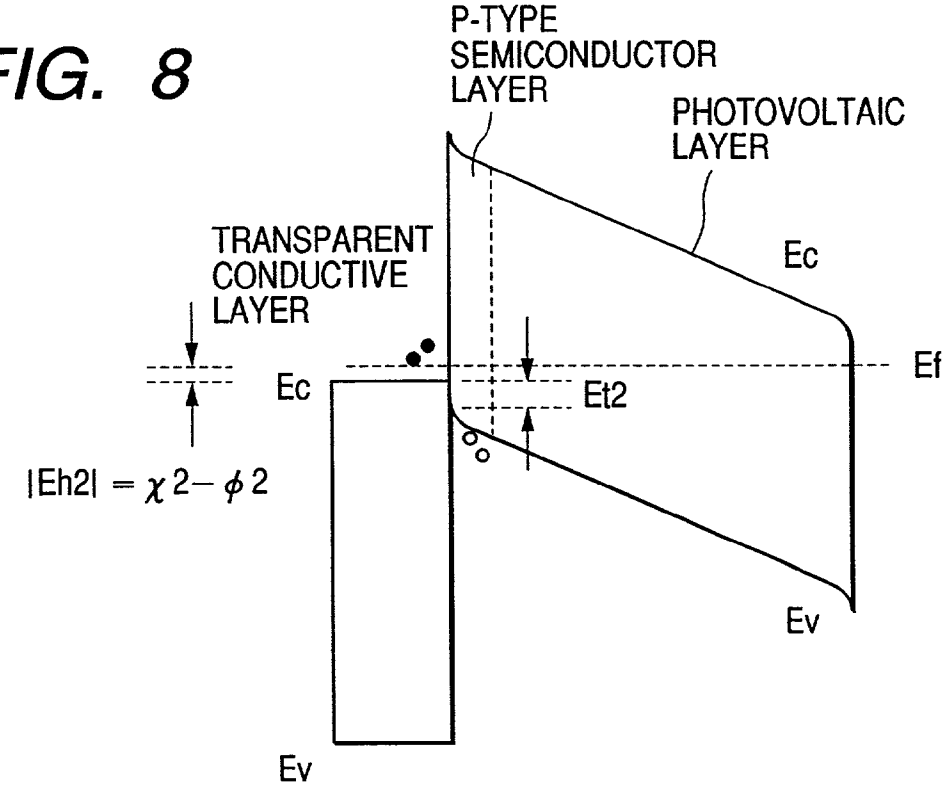
P-TYPE
SEMICONDUCTOR
LAYER
PHOTOVOLTAIC
LAYER
Ec
TRANSPARENT
CONDUCTIVE
LAYER
Ef
Ec
Et2
|Eh2| = χ2 − φ2
Ev
Ev

FIG. 9

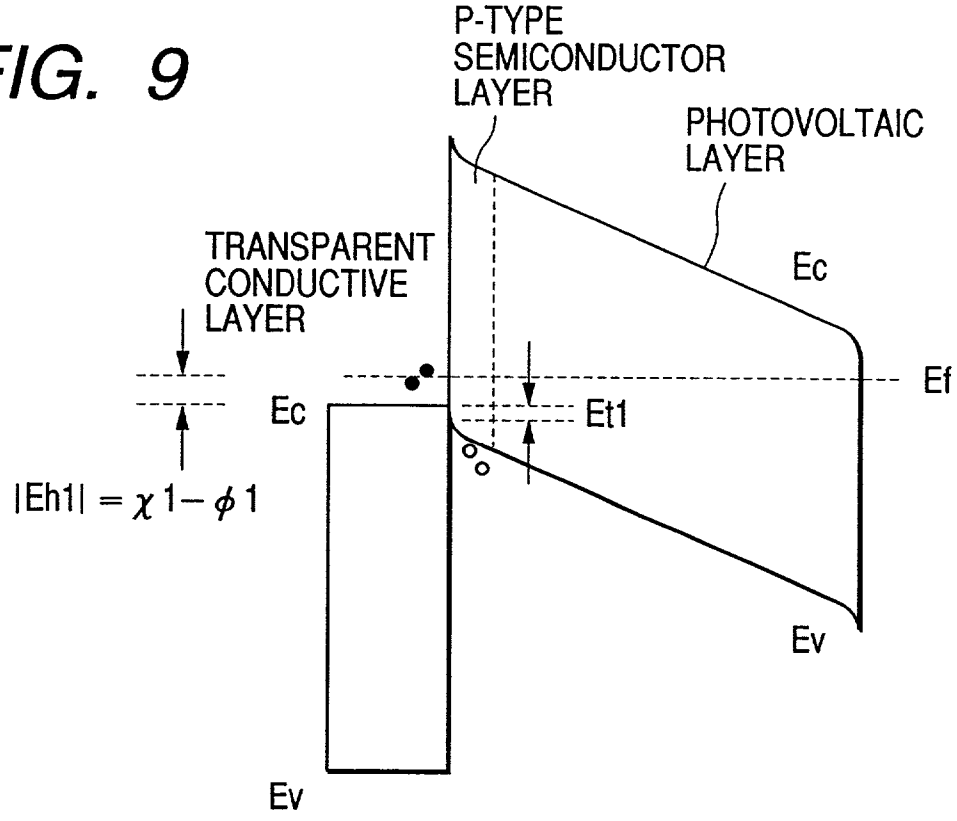
P-TYPE
SEMICONDUCTOR
LAYER
PHOTOVOLTAIC
LAYER
TRANSPARENT
CONDUCTIVE
LAYER
Ec
Ef
Et1
Ec
|Eh1| = χ1 − φ1
Ev
Ev

FIG. 10

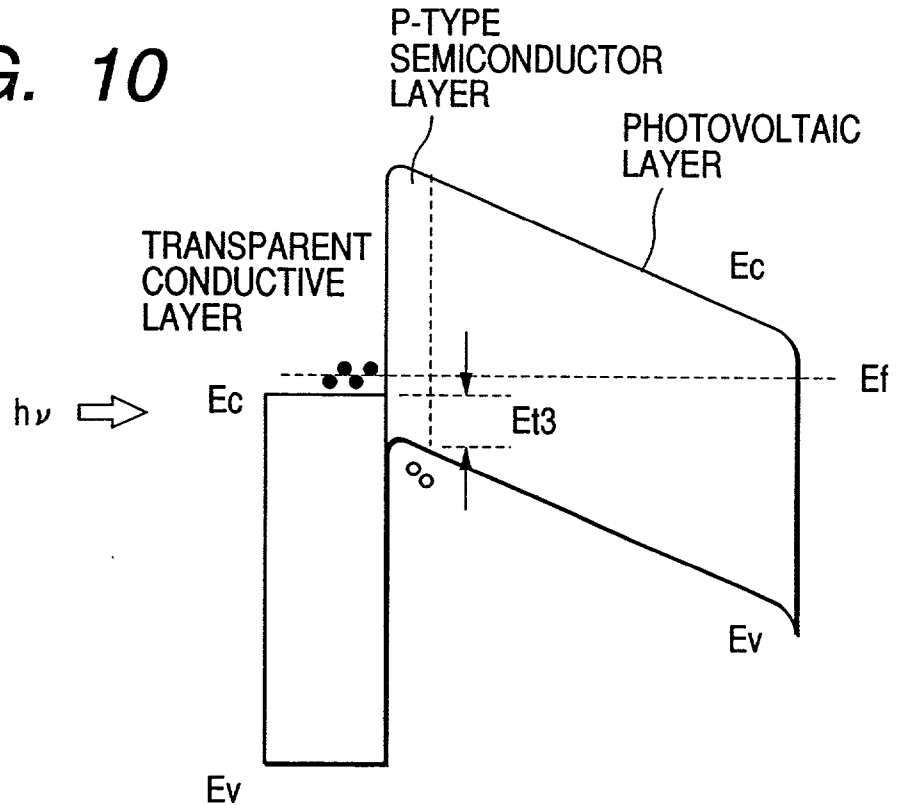
P-TYPE
SEMICONDUCTOR
LAYER
PHOTOVOLTAIC
LAYER
TRANSPARENT
CONDUCTIVE
LAYER
Ec
Ef
hν
Ec
Et3
Ev
Ev

FIG. 11

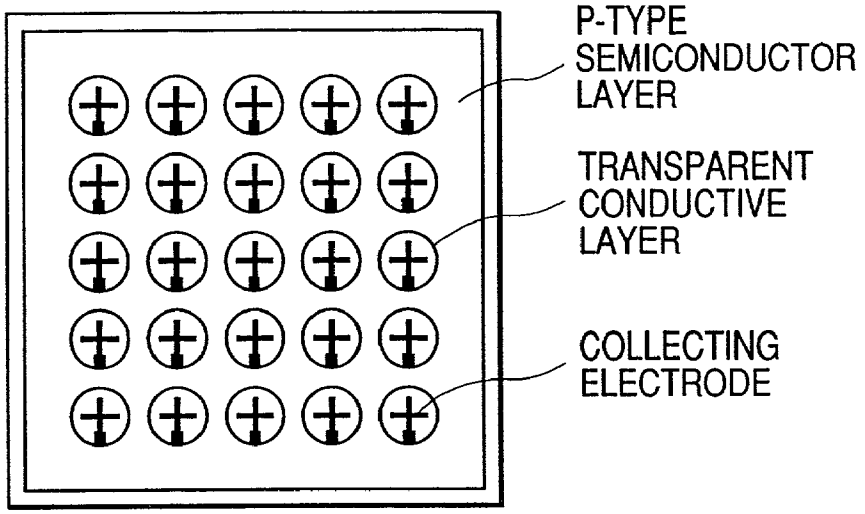
P-TYPE
SEMICONDUCTOR
LAYER
TRANSPARENT
CONDUCTIVE
LAYER
COLLECTING
ELECTRODE

FIG. 12

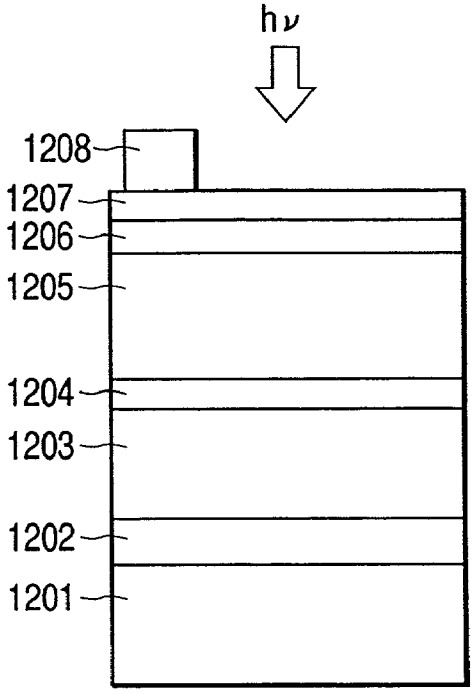
hν
1208
1207
1206
1205
1204
1203
1202
1201

FIG. 13

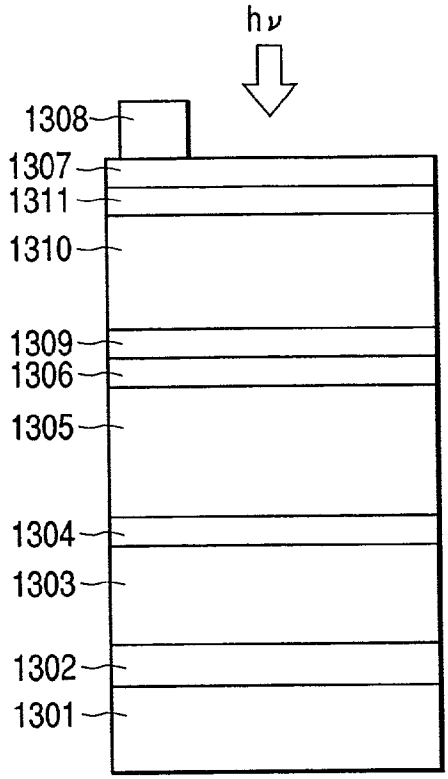

FIG. 14

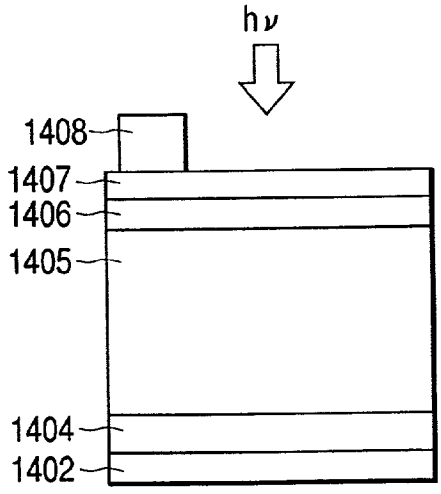

FIG. 15

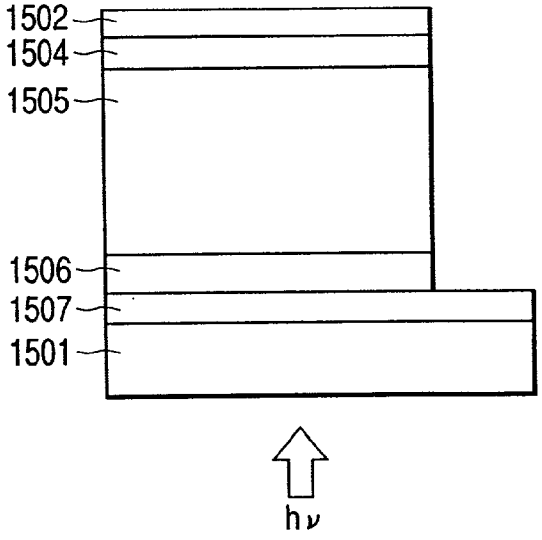

PHOTOVOLTAIC ELEMENT

BACKGROUND OF THE INVENTION

[0001] Field of the Invention

[0002] The present invention relates to a transparent conductive layer on the light incident side of a solar cell, a photosensor, or other photovoltaic element. The present invention relates in particular to those technologies which enhance the photoelectric conversion efficiency of photovoltaic elements and those technologies which increases long-term stability by inhibiting light degradation and heat degradation. The present invention relates also to improvements of cost- efficiency of photovoltaic elements.

[0003] Recently, many houses are mounted with solar cells on their roof and have them connected to the general power system so as to meet power requirement as much as possible. However, the power generation cost with solar cells is still high, which prohibits large-scale pervasion.

[0004] Although the employment of amorphous silicon-based thin-films as photovoltaic layers is said to be effective in improvement of the cost efficiency of solar cells, those thin-films have a low photoelectric conversion efficiency (conversion efficiency) as compared to crystalline solar cells and also suffer from decreases in the conversion efficiency when exposed to light irradiation, i.e. light degradation. With this, most of the past researches so far pronounced on the solar cells employing amorphous silicon-based thin-films, i.e. amorphous solar cells, have been concerned about two respects, i.e. "how to increase the conversion efficiency" and "how to decrease the light degradation".

[0005] So far, reportedly, transparent conductive layers could have been improved to obtain high-efficiency photovoltaic elements, i.e. solar cells. For example, according to Japanese Patent Application Laid-Open No. 8-77845, indium tin oxide (ITO) is formed and then exposed to a corpuscular beam of an inert gas to promote its own crystallization, thus obtaining low-resistivity, high-transmittance ITO Thin-films. Also, according to another Japanese Patent Publication No. 7- 84651, the crystallinity of ITO is controlled such that the <111> axis orientates perpendicularly to the substrate surface, thus making a trigonometric cone of the ITO surface in geometry to decrease reflection loss and improve short-circuit current and also to improve the conversion efficiency. Also, according to another Japanese Patent Application Laid-Open No. 9-78236, ITO thin-films are formed with xenon gas instead of argon gas to enhance a carrier density, thereby obtaining low-resistance ITO thin-films at a relatively low substrate temperature.

[0006] Besides, an attempt has been made to form transparent thin-films into a stack structure. For example, according to another Japanese Patent Publication No. 7-111482, transparent thin-films having different refractive indexes are stacked to obtain better reflection-preventing thin-films in a visible ray region of 450 to 650 nm. Those thin-films, however, are formed into a stack structure comprising non-conductive thin-films.

[0007] According to another Japanese Patent Application Laid-Open No. 8-43840, a plurality of high-carrier-density Thin-films (ITO:SnO_2, 10% by weight (wt %) and high-carrier-mobility thin-films (ITO:SnO_2, 0.3 wt %) are stacked and annealed, to obtain transparent conductive layers for LCD having a sheet resistivity of 5.4 $\Omega/\square$.

[0008] Recently on the other hand, such solar cells comprising single cells using uc-Si:H thin-films as the i-type layer are reported that have a high conversion efficiency and no light degradation. This solar cell is attracting the world attention as an alternative to such a type of a solar cell that employs an a-SiGe:H thin-film as the i-type layer. The uc-Si:H thin-film eliminates light degradation inherent to amorphous silicon-based thin-films such as a-SiGe:H thin-films and, moreover, need not use costly material gases such as German gas (GeH_4). In addition, this pc-Si:H thin-film does not have a high absorption coefficient as compared to a-SiGe:H thin-films but has a possibility to gain a short-circuit current (Jsc) almost like a-SiGe:H single cells by providing 2 μm or larger thin-film thickness of the i-type layer. One example of reports to that effect is MRS Symposium Proceeding Vol. 420, Amorphous Silicon Technology, 1996, pp. 3-13, "On the Way Towards High Efficiency Thin-Film Silicon Solar Cells by the Micromorph Concept", J. Meier et al., where solar cells are reported that have the i-type layer comprised of microcrystalline silicon. This solar cell is made by the VHF plasma enhanced CVD method using a frequency of 110 MHz, achieving a conversion efficiency of 7.7% for single cells having one pin junction. This single cell has a great advantage of having no light degradation. Also, by further stacking thereon another pin junction containing amorphous silicon-based thin-film as an i-type layer to make a stack cell, a conversion efficiency of 13.1% is attained. However, its light degradation rate is still high, almost the same as that for conventional amorphous silicon-based solar cells.

[0009] The inventors have made sure of such a time-wise phenomenon that indium tin oxide (ITO) thin-films have a higher resistivity with a rising temperature in the air. The inventors have also found that as light irradiation continues, a photovoltaic element using such ITO thin-films as transparent conductive layers has a higher temperature of itself and a higher resistivity of the transparent conductive layer and also a lower fill factor, short-circuit light current, and conversion efficiency. For example, in an embodiment of Japanese Patent Application Laid-Open No. 8-56004, the vacuum evaporation method by use of electron beam is used to form transparent conductive layers comprised of ITO on a substrate. Also, in an embodiment of Japanese Patent Application Laid-Open No. 7-297428, the evaporation method is used to form transparent conductive layers comprised of ITO on a photovoltaic layer. Those photovoltaic elements having ITO thin-films formed by the vacuum evaporation method have a high initial conversion efficiency but, when exposed to intense light irradiation (e.g., 100 mW/cm^2), has a higher resistivity of the ITO thin-films and a lower conversion efficiency as time passes. Also, according to Japanese Patent Application Laid-Open No. 8-43840, a plurality of high-carrier-concentration thin-films (ITO:SnO_2, 10 wt %) and high-carrier-mobility thin-films (ITO:SnO_2, 0.3 wt %) are stacked and then annealed, thereby obtaining low-resistivity transparent conductive layers for liquid crystal displays. However, when the above-mentioned thin-films are stacked on a photovoltaic layer and annealed, dopants such as phosphorus or boron are mutually diffused, thereby posing a problem of lowering in open

circuit voltage. Moreover, the light transmittancy (short-circuit current) was not high enough as required for photovoltaic elements.

[0010] In an example of Japanese Patent Application Laid-Open No. 6-5893, ITO is formed on a photovoltaic layer (pin layer) by the sputtering method. However, it suffers from a respect that the short-circuit current Jsc is small for single cells employing an a-SiGe:H thin-film as the i-type layer. As against this, researches by the inventors have shown that a certain type of ITO thin-film formed by the sputtering method has a very high thermal stability, having a change rate of resistivity of approximately 1.1 even over a time lapse of 3000 hours at a temperature of 120° C. The research by the inventors have shown also that a photovoltaic element having ITO thin-films formed on its photovoltaic layer by the sputtering method suffers from a respect that its short-circuit current is smaller than that of a photovoltaic element having ITO thin-films formed on its photovoltaic layer by the vacuum evaporation method. In addition, it has another problem that by the sputtering method, plasma comes in a high energy state to damage photovoltaic elements, thereby increasing the leakage current and decreasing the open circuit voltage. In an even worse case, it suffers from a respect that photovoltaic elements may be short-circuited. However, the photovoltaic element having ITO thin-films formed by the sputtering method has also advantages such as a high fill factor and a very excellent heat resistance.

SUMMARY OF THE INVENTION

[0011] One object of the present invention is to provide a photovoltaic element that has a high conversion efficiency and, the conversion efficiency of which does not decrease so much even when exposed to intense light for a long time. Another object of the present invention is to eliminate the decrease in the conversion efficiency due to a rise in the temperature of a photovoltaic element caused by the irradiation of intense light.

[0012] A still another object of the present invention is to improve the thermal stability of the conversion efficiency of photovoltaic elements having ITO thin-films formed on their photovoltaic layers.

[0013] As a means to solve the above-mentioned problems, the present invention provides a photovoltaic element having a p-type semiconductor layer and a transparent conductive layer comprised of indium tin oxide (ITO) junctioned face-to-face, wherein the transparent conductive layer comprises a plurality of layers and a sum of the content of tin oxide of the layer and that of tin which is the closest to the junction surface between the above-mentioned p-type semiconductor layer and transparent conductive layer of the plurality of layers is smaller than the sum of that for the other layers.

[0014] Indium tin oxide (ITO) contains mainly indium atoms, tin atoms, and oxygen atoms. Those indium atoms and tin atoms exist respectively in the state of indium oxide or another state such as an indium simple substance and the state of tin oxide or another state of a tin simple substance. The "sum of the content of tin oxide and that of tin" as referred to in the present invention means, in terms of oxide, a sum of the mole concentration of tin oxide and that of tin present in the state of tin oxide such as a tin simple substance. In other words, the "sum of the tin oxide content and the tin content" means the value of a content of tin oxide calculated from an amount of tin atoms on the assumption that all of the tin exists in the state of tin oxide and all of the indium exists in indium oxide.

[0015] Such a value can be obtained by, for example, determining the concentration of tin atoms by the inductive coupling plasma emission (ICP) method etc. and converting it in terms as oxide. If in this case the amount of tin present in a state other than tin oxide in the ITO is negligible, the "sum of tin oxide content and tin content" may be taken to be "tin oxide content".

[0016] In this case, it is preferable that the sum of content of tin oxide and that of tin of a layer which is the closest to the above-mentioned junction surface be 10 mole % or less.

[0017] It is also preferable that the sum of tin oxide content and tin content for such a layer that has the largest sum of contents of tin oxide and tin of the above-mentioned plurality of layers be between 12 mole % and 30 mole %, both inclusive.

[0018] It is also preferable that the thickness of the layer closest to the above-mentioned junction surface be a half or less of the thickness of the entire transparent conductive layer.

[0019] It is also preferable that the thickness of the layer that has the largest sum of tin oxide content and tin content of the above-mentioned plurality of layers be a half or more of the thickness of the entire transparent conductive layer.

[0020] As another means to solve the above-mentioned problems, the present invention provides a photovoltaic element having a p-type semiconductor layer and a transparent conductive layer comprised of indium tin oxide (ITO) junctioned face-to-face, wherein the sum of the content of tin oxide and that of tin within the transparent conductive layer continuously changes in the film-thickness direction, coming in a minimum at the junction surface between the above-mentioned p-type semiconductor layer and transparent conductive layer.

[0021] In this case, it is preferable that the sum of a tin oxide content and a tin content within the transparent conductive layer on the above-mentioned junction surface be 10 mole % or less.

[0022] It is also preferable that the sum of a tin oxide content and a tin content of the region that has the largest above-mentioned sum of the above-mentioned plurality of layers be between 12 mole % and 30 mole %, both inclusive.

[0023] It is also preferable that the region whose sum of a tin oxide content and tin content in the above-mentioned transparent conductive layer is 10 mole % or less occupy a half or less of the entire transparent conductive layer.

[0024] It is also preferable that the region whose sum of tin oxide content and tin content in the above-mentioned transparent conductive layer is 12 mole % or larger occupy a half or more of the entire transparent conductive layer.

[0025] Another means to solve the above-mentioned problems, the present invention provides a photovoltaic element in a thermal equilibrium state having a p-type semiconductor layer and a transparent conductive layer comprised of indium tin oxide (ITO) junctioned face-to-face, wherein the lower end of the conduction band of the transparent con-

ductive layer changes in the layer-thickness direction and also the difference between the level of the lower end of the conduction band of the transparent conductive layer in the vicinity of the junction surface between the p-type semiconductor layer and the transparent conductive layer and the Fermi level is larger than an average difference over the entire area of the transparent conductive layer.

BRIEF DESCRIPTION OF THE DRAWINGS

[0026] **FIG. 1** shows a schematic partial cross sectional view of a configuration of an photovoltaic element according to the present invention and a layer-thickness directional distribution of a sum of tin oxide content and a tin content;

[0027] **FIG. 2** shows a schematic partial cross sectional view of another configuration of an photovoltaic element according to the present invention and a layer-thickness directional distribution of a sum of tin oxide content and a tin content;

[0028] **FIG. 3** shows a schematic partial cross sectional view of a configuration of an conventional photovoltaic element and a layer-thickness directional distribution of a sum of tin oxide content and a tin content;

[0029] **FIG. 4** shows a schematic partial cross sectional view of another configuration of an photovoltaic element according to the present invention and a layer-thickness directional distribution of a sum of tin oxide content and a tin content;

[0030] **FIG. 5** shows a schematic partial cross sectional view of another configuration of an photovoltaic element according to the present invention and a layer-thickness directional distribution of a sum of tin oxide content and a tin content;

[0031] **FIG. 6** is a diagram of a band of a photovoltaic element according to the present invention prior to junction;

[0032] **FIG. 7** is a diagram of a band of a photovoltaic element according to the present invention;

[0033] **FIG. 8** is a diagram of a band of a conventional photovoltaic element;

[0034] **FIG. 9** is a diagram of a band of another conventional photovoltaic element;

[0035] **FIG. 10** is a diagram of a band of another conventional photovoltaic element;

[0036] **FIG. 11** is an outer appearance view of a sample solar cell used in experimental examples and embodiments;

[0037] **FIG. 12** is a schematic cross sectional view of an embodiment of a photovoltaic element according to the present invention;

[0038] **FIG. 13** is a schematic cross-sectional view of another embodiment of a photovoltaic element according to the present invention;

[0039] **FIG. 14** is a schematic cross-sectional view of another embodiment of a photovoltaic element according to the present invention; and

[0040] **FIG. 15** is a schematic cross-sectional view of another embodiment of a photovoltaic element according to the present invention.

DESCRIPTION OF THE PREFERRED EMBODIMENTS

[0041] To improve the conversion efficiency of photovoltaic elements, it is critical to decrease the specific resistance of and increase the transmittance of the transparent conductive layer. However, the inventors have found as a result of researches "when the transparent conductive layer and the photovoltaic layer have reached a relatively high level in quality, improvements in the characteristics of the simple substances of the transparent conductive layer such as specific resistance and transmittance do not necessarily lead to improvement in the characteristics of the photovoltaic element". The inventors have concluded that when a semiconductor layer in contact with the transparent conductive layer is in particular of a p-type, its junction state is very important. The inventors have also found that when the transparent conductive layer comprised of ITO in junction with semiconductor layers is exposed to high temperatures such as 60° C., the specific resistance may sometimes rise as time passes. And the extent of a rise in temperature is found to be correlated with the sum of a tin oxide content and a tin content of the transparent conductive layer comprised of ITO, in such manner that with smaller contents of about 5 mole % the specific resistance rises as time passes and with larger contents of about 15 mole %, the specific resistance comes to have an excellent thermal stability. It has been found however that if a highly-heat-stable transparent conductive layer having a large sum (which may sometimes be abbreviated simply as tin concentration hereinafter) of a tin oxide content and tin content is junctioned as it is with a photovoltaic layer, the conversion efficiency degrades a little. Discussion on the conditions for forming the transparent conductive layer has concluded that the conversion efficiency in this case extremely rarely becomes higher than that with the case of junction with a transparent conductive layer having a lower tin concentration.

[0042] The present invention has been worked out based on those experimental results, resulting in a photovoltaic element having an improved junction between transparent conductive layers and photovoltaic layers as well as a high conversion efficiency and a good thermal stability.

[0043] **FIG. 3** is a partial cross-sectional view of a conventional photovoltaic, which has in it a photovoltaic layer comprised of pn junctions or pin junctions (not shown) and a transparent conductive layer **302** comprised of ITO in contact with a p-type semiconductor layer **301**. This transparent conductive layer has a constant concentration (C_{31}) of tin. In this case, the concerned junction may well be shown in the band diagram in **FIGS. 8 and 9**. ITO, having its Fermi level above the lower end of conduction band, is so called a degenerated semiconductor. The transparent conductive layer shown in **FIG. 3** is considered to have a smaller work function ϕ with a smaller concentration of tin and a larger work function with a larger concentration of tin (Report of Research Laboratory of Engineering Shibaura Institute of Technology, Vol. 3, 1988, pp. 35-55). If the electron affinity x is supposed to be the same as each other, the absolute value of a difference between the level (Ec) of the lower end of the conduction band and the Fermi level (Ef) is smaller in the case of a larger concentration of tin (**FIG. 8**, Eh2) than in the case of a smaller concentration of tin (**FIG. 9**, Eh1), i.e. Eh1>Eh2.

[0044] Also, the tunnel current is considered to be larger with a smaller band gap (Et) concerned with the tunnel current and smaller with a larger value of Et. The above consideration leads to a supposition of the following relationship:

$$Et1<Et2$$

[0045] Therefore, a band gap concerned with tunnel current is smaller in the case of **FIG. 9** with a smaller concentration of tin, thus resulting in a larger flow tunnel current. If a tunnel current is small, the photovoltaic effect generated at the transparent conductive layer and the p-type semiconductor layer cannot be neglected. Therefore, it is considered that such a photovoltaic element is preferable to that of a type shown in **FIG. 9**, which has a larger tunnel current, i.e. having a small or zero concentration of tin. Actually, measurement of the solar cell characteristics of an amorphous silicon solar cell having pin junctions has shown that the type shown in **FIG. 9** is preferable in terms of open circuit voltage (Voc), short-circuit current (Jsc), and photo-electric conversion efficiency (η).

[0046] However, the photovoltaic element having a transparent conductive layer shown in **FIG. 9** suffers from, when exposed to a high temperature such as about 90° C. for a long time, increases in the specific resistance and sheet resistance as well as degradations in the solar cell characteristics, particularly fill factor (FF). However, the photovoltaic element shown in **FIG. 8** has, as compared to that in **FIG. 9**, slightly degraded open circuit voltage (Voc), short-circuit current (Jsc), and photoelectric conversion efficiency (η), but its transparent conductive layer has an excellent thermal stability, so that even if exposed to a high temperature such as about 120° C., its specific resistance and sheet resistance are very stable and also that open-circuit voltage (Voc), short-circuit current (Jsc), and photoelectric conversion efficiency (η) are also thermally stable.

[0047] The present invention makes use of advantages of respective types shown in **FIGS. 8 and 9** and, at the same time, eliminates their disadvantages. **FIG. 1** is schematic partial cross-sectional view of one embodiment of the photovoltaic element according to the present invention, in which example, a transparent conductive layer **102** consists of a stack of two layers. That is, in the case of **FIG. 1, a** first transparent conductive layer **103** and a second transparent conductive layer **104** are sequentially stacked on a p-type semiconductor layer **101**, with the first transparent conductive layer **103** having a concentration smaller than that of the second transparent conductive layer **104**. **FIGS. 6 and 7** show band diagrams of the photovoltaic element shown in **FIG. 1**. In a first transparent conductive layer, which has a smaller concentration of tin, the energy gap concerned with the tunnel current Et1 is relatively small. Therefore, the tunnel current becomes larger to inhibit undesired photovoltaic effect from being generated, thereby providing better open-circuit voltage (Voc), short-circuit current (Jsc), and photoelectric conversion efficiency (i). **FIG. 2** is a schematic partial cross-sectional view of one embodiment of the photovoltaic element according to the present invention, in which on a p-type semiconductor layer **201** is formed a transparent conductive layer **202** comprised of a first transparent layer **203**, a second transparent conductive layer **204**, and a third transparent conductive layer **205**.

[0048] In the conventional photovoltaic elements, it is considered that if a great deal of tin oxide or tin is present near the interface, the concerned region has a larger carrier concentration, so that caused by mirror image force, the energy band is made to curve as **FIG. 10**. With this, essentially the energy gap Et3 concerning the tunnel current becomes even larger, decreasing the tunnel current with loss which is as much as photovoltaic effect. It is considered that photovoltaic elements according to the present invention have a relatively small concentration of tin concentration in the first transparent conductive layer near the junction surface and so have a smaller carrier concentration, eliminating undesired curves of the band near the junction surface of the p-type semiconductor layer, as shown in **FIG. 10**. Therefore, the tunnel current becomes larger, thus giving excellent open-circuit voltage, short-circuit current, and photoelectric conversion efficiency of the photovoltaic elements according to the present invention.

[0049] Moreover, since the second transparent conductive layer having a larger concentration of tin is stacked on the first transparent conductive layer, an excellent thermal stability can be obtained. Moreover, since the refractive index n2 of the second transparent conductive layer is larger than the refractive index n1 of the first transparent conductive index, when the refractive index of a material of the photovoltaic layer is larger than n2, the light trapping effect increases to further increase the short-circuit current. Also, since the first transparent conductive layer functions as a buffer layer against the internal stress, the transparent conductive layers of a photovoltaic element according to the present invention is very difficult to be peeled off. Since the tin concentration particularly near the junction surface is small to promote stress relaxation, the interface state is very low, thus providing excellent photoelectric characteristics. Also, according to the present invention, the specific resistance is smaller at the transparent conductive layers (the second transparent conductive layer **124** in **FIG. 1** and the third transparent conductive layer **205** in **FIG. 2**) distant from the junction surface than at those (the first transparent conductive layers **103** and **203** in FIGS. **1** and **2**) near the junction surface, so that light carriers generated from the photovoltaic layer move in the layer-thickness direction inside the transparent conductive layer near the junction surface and in the into-the-surface direction inside the transparent conductive layer distant from the junction surface. Therefore, the interaction due to the movement of carriers near the junction surface or inside the p-type semiconductor layer is decreased, thus increasing the tunnel current.

[0050] The above-mentioned effects can be obtained mostly the same with a photovoltaic element shown in **FIG. 2** that has a three-layer stacked transparent conductive layer and also that the tin concentration starts to increase at the junction surface. Also, the above-mentioned effects can be exerted further more for photovoltaic elements shown in **FIGS. 4 and 5** that the tin concentration starts to increase continuously at the junction surface. That is, by continuously changing the concentration of tin oxide or tin, the interface between the first and second transparent conductive layers can be eliminated, thus providing an advantage in the case where an interface state is present at the concerned interface. Since there is no interface state, power loss due to increases in resistance is eliminated. Note here that **FIGS. 4 and 5** are both schematic partial cross-sectional views showing the embodiments of the photovoltaic element according to the present invention.

[0051] Also, according to the present invention, transparent conductive layers may be stacked on p-type semiconductor layers or vice versa. In addition, the light incidence direction may be from the side of the transparent conductive layer or the photovoltaic layer, to exert the effects by the present invention.

[0052] One preferred embodiment of the present invention features that the concentration of tin of the layer closest to the junction surface is 10 mole % or less. Another embodiment wherein the tin concentration changes continuously features that the concerned concentration becomes a minimum at the junction surface, i.e. 10 mole % or less. With this, an energy gap related to the tunnel current becomes even smaller to further increase it, thus exerting the above-mentioned effects even more conspicuously.

[0053] Another preferred embodiment of the present invention features that the tin maximum concentration of any layer is between 12 mole % and 30 mole %, both inclusive. Also, another preferred embodiment in which the tin concentration changes continuously features that the tin concentration in its maximum region is between 2 mole % and 30 mole %, both inclusive. With this, the thermal stability of photovoltaic elements when exposed to a high temperature can be further improved. This improvement exerts the above-mentioned effects even more conspicuously.

[0054] Another preferred embodiment of the present invention features that the layer thickness of a region where the tin concentration near the junction surface is 10 mole % or less is a half or less of the entire thickness of the ITO layer. With this, the thermal stability of photovoltaic elements when exposed to a high temperature can be further improved. This improvement exerts the above-mentioned effects even more conspicuously.

[0055] Another preferred embodiment of the present invention features that the layer thickness in a region where the tin concentration is 12 mole % or higher is a half or larger of the entire thickness of the ITO layer. With this, the thermal stability of photovoltaic elements when exposed to a high temperature can be further improved. This improvement exerts the above-mentioned effects even more conspicuously.

[0056] Another preferred embodiment of the present invention features that the film thickness of transparent conductive layers is adjusted so that the intensity of reflected light may be a minimum at the wavelength at which the intensity of illumination light becomes a maximum. With this, the short-circuit current for photovoltaic elements is increased.

[0057] (Configuration of Transparent Conductive Layers)

[0058] The transparent conductive layers employed in the present invention are comprised of indium tin oxide (ITO) and may be in a polycrystalline, microcrystalline, or amorphous state. Of these states, the crystalline state makes it possible to obtain a lower specific resistance and a higher transmittance. A forming temperature of 100° C. or higher is preferable in order to form crystalline indium tin oxide layers. To further improve the transmittance, the forming temperature should preferably be 150° C. or higher. When the underlying layer is not a p-type semiconductor layer when forming transparent conductive layers, the forming temperature should preferably be 300° C. or higher. If the underlying layer is a p-type semiconductor layer, it is necessary to optimize the forming temperature for the concerned layers in order to obtain even a little higher conversion efficiency. Generally, however, an appropriate forming temperature for the underlying p-type semiconductor layers is 400° C. or lower. This is because that temperature is important to prohibit the dopants etc. in the p-type semiconductor layer from being mutually diffused into other layers in order to increase the open-circuit voltage. It is also preferable to form this layer at a highest possible temperature to make its surface uneven, thus making the best use of the light trapping effect. It is also preferable to adjust the film thickness so that the reflection becomes a minimum at a wavelength at which the illumination light intensity becomes a maximum, thereby absorbing the illumination light into the photovoltaic layer as much as possible. When transparent conductive layers according to the present invention are used in a crystalline state, their orientation should preferably be a (100) or (111) surface in order to grow larger crystal particles even with a lower specific resistance and a higher transmittance. With this, it is also easy to form uneven structures in the surface.

[0059] (How to Form Transparent Conductive Layers)

[0060] The methods of forming transparent conductive layers in the photovoltaic element according to the present invention includes the spray method, the CVD method, the application method, the resistance heating vacuum evaporation method, and the sputtering method, of which the resistance heating vacuum evaporation method, the electron-beam vacuum evaporation method, or the sputtering method is the most appropriate one because it enables forming good junction surfaces with semiconductor layers. When using the resistance heating vacuum evaporation method or the electron-beam vacuum evaporation method, it is preferable to evaporate a metal evaporation source containing indium and tin at a pressure of 7×10^{-2} Pa as heating the source subjected to oxygen gas. If compared at the same temperature, however, the vapor pressure of tin is much lower than that of indium, so that in order to provide an approximately 1 mole % of tin concentration in transparent conductive layers, their weight ratio needs to be In:Sn=1:1 or so, while in order to provide an approximately 10 mole % of tin concentration, their weight ratio needs to be In:Sn=1:10 or so. The sputtering method, particularly the DC magnetron sputtering method is optimal because it provides a higher deposit rate and better junction surfaces. Preferably, the forming temperature is 150° C. or higher and the target voltage, −200 V to −500 V or so. Also, as a sputtering gas, a mixture of argon and oxygen as well as neon, helium, and other light gases is preferable to reduce the plasma-damages at the junction surface. In addition, the substrate may be electrically floated or a bias may be adjusted so as to control electron current or ion current flowing into the substrate. A voltage of −50 V or higher is preferable and especially preferable is a voltage of +200 V or so in order to reduce ion current and plasma-damages.

[0061] In order to change the tin concentration in the layer-thickness direction, electric power applied to the target or the evaporation source may be controlled independently. When the sputtering method is employed, by preparing both a target comprised of indium oxide and another target comprised of tin oxide and tin beforehand, electric power

onto the tin oxide target should be increased in order to provide a higher content of tin oxide. In order to provide a higher content of tin, on the other hand, electric power onto the tin target should be increased. When the resistance heating vacuum evaporation is employed, by preparing both an indium evaporation source and a tin evaporation source, the temperature for the tin evaporation source should be increased in order to provide a higher concentration of tin.

[0062] (Photovoltaic Layer)

[0063] The photovoltaic layer may be of any junction aspect as long as its configuration will generate photovoltaic effect when exposed to light irradiation. The junction aspects preferred include the pn junction, pin junction, p^+ p^- n^+ junction, and p^+ n^- n^+ junction. The materials for photovoltaic layers include Si, Ge, SiGe, SiC, CdS, CdTe, CdSe, $Cd_xZn_{1-x}S$, GaAs, $Ga_xAl_{1-x}As$, $GaInP_2$, InP, $CuInSe_2$, $CuIn_xGa_{1-x}Se_2$, Cu_2S, ZnO, Zn_3P_2, and Se. The junction may be formed in a homostructure using the same kind of materials or a heterostructure using different kinds of materials. The state of the materials also may be monocrystal, polycrystal, microcrystalline, or amorphous, sometimes coming in a hetero-junction of polycrystal and amorphous states. The photovoltaic layers of the present invention may have a plurality of junctions. Those junctions may also be formed in series or have insulating layers inserted between themselves. They also may have different kinds of junctions such as a pn junction and a pin junction.

[0064] The methods of forming photovoltaic layers include the plasma-enhanced CVD method, the photo-assisted CVD method, the thermal CVD method, MOCVD method, the MBE method, the gas diffusion method, the solid-phase diffusion method, the liquid-phase growth method, the ion implantation method, the resistance heating vacuum evaporation method, the spray method, the sputtering method, and the electro-deposition method, of which however the most appropriate method must be selected depending on materials and junction aspects to be employed. Also a plurality of methods may be used when forming junctions for the photovoltaic layer.

[0065] In order to form junctions by depositing thin-films of Si, Ge, SiGe, or SiC, the plasma enhanced CVD method, the photo-assisted CVD method, and the thermal CVD method are preferable. In order to form junctions within the substrate, the gas diffusion method, the solid-phase diffusion method, and the ion implantation method are preferable. In order to form the i-layer in particular, the RF plasma-enhanced CVD method using a frequency of 1 to 30 MHz, the VHF plasma-enhanced CVD method using a frequency of 30 MHz to 0.5 GHz, and the microwave plasma-enhanced CVD method using a frequency of 0.5 GHz to 10 GHz are preferable. In order to form junctions by depositing thin-films of CdS, CdTe, CdSe, or $Cd_xZn_{1-x}S$, the resistance heating vacuum evaporation method, the MBE method, the sputtering method, the electro-deposition method, the plasma-enhanced CVD method, and the photo-assisted CVD method are preferable. In order to form junctions by depositing thin-films of GaAs, $Ga_xAl_{1-x}As$, $GaInP_2$, or InP, the MBE method, the MOCVD method, and the liquid-phase growth method are preferable, while in order to form junctions within the substrate, the gas diffusion method, the solid-phase diffusion method, and the ion implantation method are preferable. In order to form junctions by depositing thin-films of $CuInSe_2$, $CuIn_xGa_{1-x}Se_2$, Cu_2S, or ZnO, the resistance heating vacuum evaporation method, the MBE method, and the sputtering method are preferable. In order to form junctions by depositing Zn_3P_2 thin-films, the ICB method and the MOCVD method are preferable. In order to form junctions by depositing Se thin-films, the resistance heating vacuum evaporation method and the sputtering method are preferable.

[0066] After the junctions are formed by above-mentioned methods, annealing may be carried out for re-crystallization or improvement of the junction quality.

[0067] (p-type Semiconductor Layer)

[0068] The p-type semiconductor layer is junctioned with transparent conductive layers, being comprised of a material having the p-type conductivity of many photovoltaic materials used for the photovoltaic layer. The material may come in Si, Ge, SiGe, SiC, CdTe, GaAs, $Ga_xAl_{1-x}As$, $GaInP_2$, InP, $CuInSe_2$, $CuIn_xGa_{1-x}Se_2$, Cu_2S, Zn_3P_2, or Se. The material may also come in such a state as a monocrystalline, polycrystalline, microcrystalline, or amorphous state, so that different states of for example polycrystalline and amorphous states may be used to stack a plurality of layers.

[0069] The methods of forming p-type semiconductor layers include the plasma-enhanced CVD method, the photo-assisted CVD method, the thermal CVD method, the MOCVD method, the gas diffusion method, the solid-phase diffusion method, the liquid-phase diffusion method, the ion implantation method, the resistance heating vacuum evaporation method, the spray method, the sputtering method, and the electrodeposition method, of which however the most appropriate method must be selected depending on the material and the junction aspect to be employed. This method of forming p-type semiconductor layers is to be in accordance with the above-mentioned method of forming photovoltaic layers.

[0070] (Photovoltaic Element)

[0071] **FIG. 12** shows a schematic cross-sectional view of the specific configuration of one example of the photovoltaic element according to the present invention. **FIG. 12** illustrates a pin-type solar cell employing a non-monocrystalline silicon-based semiconductor. In **FIG. 12**, reference numeral **1201** indicates a support structure which has a function to support a photovoltaic element, coming in glass, stainless steel, heat-resistant resin sheet, etc. in material. Reference numeral **1202** indicates a reflecting layer which has functions as a back-surface electrode and also a back-surface reflecting function, coming in Ag, Al, Au, Cu, CuMg etc. in material. Reference numeral **1203** indicates a lower transparent conductive layer which has functions to prevent short-circuiting of photovoltaic layers and also a light trapping function, coming in zinc oxide, tin oxide, indium oxide, ITO etc. in material. Reference numerals **1204**, **1205**, and **1206** respectively indicate an n-type semiconductor layer, an i-type semiconductor layer, and a p-type semiconductor layer; and by junctioning these layers the pin junctions can be formed to generate photovoltaic effect. The stack structure comprised of these three types of layers is called a photovoltaic layer. The materials used for that are mentioned earlier. Reference numeral **1207** indicates a transparent conductive layer comprised of indium tin oxide, coming in a stack structure consisting of two layers or more in which

the tin concentration changes in the layer-thickness direction. This transparent conductive layer has a function to lead a larger amount of light to the photovoltaic layer and another function to lead light carriers to the collecting electrode effectively, i.e. with a smaller power loss. Reference numeral **1208** indicates the collecting electrode which has a function to effectively lead light carriers outside and another function to lead light to the photovoltaic layer effectively. The materials to be employed include Ag, Al, Au, Cu etc.

[**0072**] **FIG. 13** is a schematic cross-sectional view of a photovoltaic element, which is a pinpin-type tandem non-monocrystalline silicon-based solar cell. The materials and functions of each layer are almost the same as those in **FIG. 12**.

[**0073**] In **FIG. 13**, reference numeral **1301** indicates a support structure, reference numeral **1302** indicates a reflecting layer, reference numeral **1303** indicates a lower transparent conductive layer, reference numeral **1304** indicates a first n-type semiconductor layer, reference numeral **1305** indicates a first i-type semiconductor layer, reference numeral **1306** indicates a first p-type semiconductor layer, reference numeral **1307** indicates a transparent conductive layer, reference numeral **1308** indicates a collecting electrode, reference numeral **1309** indicates a second n-type semiconductor layer, reference numeral **1310** indicates a second i-type semiconductor layer, and reference numeral **1311** indicates a second p-type semiconductor layer.

[**0074**] **FIG. 14** is a schematic cross-sectional view of another example of a photovoltaic element, which is a p^+ n^- n^+-type monocrystalline silicon-based solar cell. Reference numeral **1405** indicates an n^--type semiconductor layer consisting of an n^--type monocrystalline silicon substrate which is prepared by the pull method and then into which phosphorous (P) is doped. Reference numeral **1404** indicates an n^+-type semiconductor layer which is prepared by implanting phosphorous ions into the back surface of the concerned n^--type monocrystalline silicon substrate. Reference numeral **1406** indicates a p^+-type semiconductor layer which is prepared by implanting boron ions into the surface of the concerned n^--type monocrystalline silicon substrate. These layers indicated by reference numerals **1404**, **1405**, and **1406** will in combination generate photovoltaic effect and their stack structure is called a photovoltaic layer. Reference numeral **1402** indicates a reflecting layer which serves also as a back-surface electrode, having a function as an electrode and also as a layer to reflect light, being comprised of Al etc. Reference numerals **1407** and **1408** respectively function the same as the transparent electrode layer **1207** and the collecting electrode **1208**.

[**0075**] **FIG. 5** is a schematic cross-sectional view of another example of a photovoltaic element, which causes the light to enter from the side of a support structure **150**. The support structure **1501**, therefore, needs to be transparent. On the support structure **1501** are sequentially stacked a transparent conductive layer **1507**, a p-type semiconductor layer **1506**, an i-type semiconductor layer **1505**, an n-type semiconductor **1504**, and a reflecting layer **1502**.

[**0076**] [Experiments]

[**0077**] To investigate the effects by the present invention, a sample of such a stack structure was prepared that consists of a transparent conductive layer, a p-type semiconductor layer, and a substrate in this order.

[**0078**] (Experiment 1)

[**0079**] First, as a substrate, a stainless plate (50 mm×50 mm×1 mm (thickness)) which had undergone specular polishing was provided and on it, as a p-type semiconductor layer, a p-type microcrystalline silicon (μc-Si:H:B) was formed by the RF plasma-enhanced CVD method. On it was formed a transparent conductive layer **102** using a DC magnetron sputtering apparatus having in it four targets, as shown in **FIG. 1**. Specifically, a mask having in it 25 openings with a 6-mm diameter was placed on a p-type semiconductor layer **101** and then placed in the DC magnetron sputtering apparatus, to sequentially form a first transparent conductive layer **103** and a second transparent conductive layer **104** under such conditions as listed in Table 1. Then, the heater was turned off and, when the temperature reached approximately the room temperature, a mask having in it cross-shaped openings was placed on, to form collecting electrodes comprised of Al on the second transparent conductive layer **104**, thereby completely preparing a sample shown in **FIG. 11** as viewed from the top.

[**0080**] When the voltage-current characteristic of this sample under the dark conditions was checked, it was found to be ohmic. Also, when its voltage-current characteristic was checked by applying a light of AM 1.5 and 100 mW/cm^2, no photovoltaic effect was detected.

[**0081**] Next, In much the same manner as mentioned above, a p-type semiconductor layer **101**, a first transparent conductive layer **103**, and a second transparent conductive layer **104** were stacked on a glass-made substrate. When measured by the four-probe method, the sheet resistance of the transparent conductive layer **102** was 48.0 Ω/□. Then, the sample was placed in a high-temperature environmental testing machine held at 120° C. and allowed to stand in it for 1000 hours, whereupon the sheet resistance of the transparent conductive layer **102** was measured to be 50.8 (Ω/□). The layer forming conditions and the results are summarized in Table 1.

[**0082**] (Comparative Experiment 1-1)

[**0083**] Next, the first transparent conductive layer was checked in terms of its single-film characteristics. Like in Experiment 1, on a stainless-steel substrate was formed a p-type semiconductor layer, on which in turn was formed a transparent conductive layer with a film thickness of 60 nm, on which in turn was formed cross-shaped collecting electrodes. The voltage-current characteristic of this sample under the dark conditions was checked and found to be ohmic. When the voltage-current characteristic was checked by applying a light of AM 1.5 and 100 mW/cm^2, no photovoltaic effect was detected. Next, on a glass-made substrate was formed a p-type semiconductor layer, on which in turn was formed a first transparent conductive layer with a film-thickness of 60 nm, and then the resulting sample was measured for its sum of indium content and tin content (tin concentration) by the ICP method to be found to be 5.1 mole %. Also, the initial sheet resistance and the sheet resistance after a time lapse of 1000 hours at a temperature of 120° C. were measured like in Experiment 1, to be found to be 70.4 (Ω/□) and 85.1 (Ω/□), respectively. The layer forming conditions and the results are summarized in Table 2.

[0084] (Comparative Experiment 1-2)

[0085] Next, the second transparent conductive layer was checked for its single-film characteristics. Like in Experiment 1, on a stainless-steel substrate was formed a p-type semiconductor layer, on which in turn was formed a second transparent conductive layer with a film-thickness of 60 nm, on which in turn was formed cross-shaped collecting electrodes. The voltage-current characteristic of this sample under the dark conditions was to be a little of rectifying. Also, when checked by applying a light of AM 1.5, 100 mW/cm^2, the voltage-current characteristic was found to be generating photovoltaic effect a little. Next, on a glass-made substrate was formed a p-type semiconductor layer, on which in turn was formed a second transparent conductive layer with a film-thickness of 60 nm; and the resultant tin concentration was measured by the ICP method to be 10.3 mole %. Also, like in Experiment 1, the initial sheet resistance and the sheet resistance after a time lapse of 1000 hours at a temperature of 120° C. were measured to be 42.1 (Ω/□) and 44.3 (Ω/□) respectively The layer forming conditions and the results are summarized in Table 3.

[0086] (Experiment 2)

[0087] The same sample as that in Experiment 1 was prepared and evaluated similarly except that the first transparent conductive layer was formed by the resistance heating vacuum evaporation method and also that such a target for forming the second transparent conductive layer was employed that has a tin oxide content of 15 mole %. The conditions and the results are summarized in Table 4.

[0088] (Comparative Experiment 2-1)

[0089] Next, the first transparent conductive layer formed in Experiment 2 was checked for its single-film characteristics. Like in Comparative Experiment 1-1, on a stainless-steel substrate were formed a p-type semiconductor layer and a first transparent conductive layer, and a collecting electrode in this order to give a sample, while on a glass-made substrate were formed a p-type semiconductor layer and a first transparent conductive layer in this order to give another sample; then they were checked for their current-voltage characteristic, tin concentration, and initial sheet resistance and then underwent heat-run tests. The layer forming conditions and the results are summarized in Table 5.

[0090] (Comparative Experiment 2-2)

[0091] Next, the second transparent conductive layer formed in Experiment 2 was checked for its single-film characteristics. Like in Comparative Experiment 1-2, on a stainless-steel substrate were formed a p-type semiconductor layer, a second transparent conductive layer, and collecting electrodes to prepare a sample, while on a glass-made substrate were formed a p-type semiconductor layer and second transparent conductive layer to prepare another sample, so that these two sample were tested to determine their current-voltage characteristic and initial sheet resistance and also underwent heat run tests. The layer forming conditions and the results are summarized in Table 6.

[0092] As can be seen from these experimental examples, the transparent conductive layer having a configuration shown in **FIG. 1** of the present invention has found to form ohmic junctions with p-type semiconductor layers, to generate no photovoltaic effect, and to be excellent in thermal stability.

[0093] (Experiment 3)

[0094] The single-film characteristics were summarized for each of various values of the concentrations of transparent conductive layers. The results are summarized in Table 7. The same evaluation method was taken as Experiments 1 and 2. In this case, the layers were formed by the DC magnetron sputtering method, to change the content of tin oxide contained in a target, thereby varying the tin concentration in the transparent conductive layers. As can be seen from this table, when the tin concentration is in a range of 12 mole % to 30 mole %, both inclusive, the sheet resistance is low and the thermal stability is high.

[0095] (Experiment 4)

[0096] This experiment was conducted using a sputtering target containing metal tin. By changing the metal tin content in the target, the tin concentration in transparent conductive layers was varied. The results have shown that when the tin concentration is in a range of 12 mole % to 30 mole %, both inclusive, the sheet resistance is low and the thermal stability is high.

[0097] (Experiment 5)

[0098] This experiment was conducted on various values of the tin concentration in transparent conductive layers using the resistance heating vacuum evaporation method a:=and the electron-beam vacuum evaporation method. This experiment was carried out in the same manner as Experiment 3, except for the method of forming transparent conductive layers. The results have shown that when the tin concentration is in a range of 12 mole % to 30 mole %, both inclusive, the sheet resistance is low and the thermal stability is high irrespective of the forming method employed.

[0099] (Experiment 6)

[0100] The experiment was conducted on, as a p-type semiconductor layer, the polycrystalline $CuInSe_2$ with a film-thickness of 50 nm formed by the seleniding method. In this experiment, a stack layer comprised of Cu/In formed by the vacuum evaporation method was selenided by undergoing heat treatment in a Se vapor. First, as a substrate, a glass-made substrate on which Mo was sputtered was used; it then was heated to 450° C. at a rate of 200° C./minute, underwent the irradiation for 60 minutes by selenium vapor from a Se vapor source to form a sample, and was cooled slowly at a rate of 1° C./minute down to 300° C., whereupon the irradiation by selenium vapor was stopped. It was further cooled slowly at a rate of 1° C./minute to sequentially form 25 first transparent conductive layers with a 6-mm diameter, another 25 second transparent conductive layers, and cross-shaped Al-made collecting electrodes.

[0101] When its voltage-current characteristic under the dark conditions was checked, the sample was found to be ohmic. Also, when a light of AM 1.5, 100 mW/cm^2 was applied to check its voltage-current characteristic, the sample was found to generate no photovoltaic effect.

[0102] Next, likewise, a p-type semiconductor layer, a first transparent conductive layer, and a second transparent conductive layer were stacked on a glass-made substrate in

much the same manner as above. The sheet resistance was measured by the four-probe method and found to be 45.2 (Ω/□). Then, the sample was placed in a high-temperature environmental testing machine held at 120° C., allowed to stand there for 1000 hours, and then measured for its sheet resistance to be found to be 47.8 (Ω/□).

[0103] (Comparative Experiment 6-1)

[0104] Next, the first transparent conductive layer was checked for its single-film characteristics. Like in Experiment 6, on a Mo/glass-made substrate was formed a p-type semiconductor layer comprised of $CuInSe_2$ in the same manner as Experiment 6, on which in turn was formed a first transparent conductive layer with a 60-nm thickness in the same manner as Comparative Experiment 1-1, on which in turn was formed cross-shaped collecting electrodes. The sample was checked for its voltage-current characteristics under the dark conditions and found to be ohmic. When checked also for its voltage-current characteristics after the irradiation by a light of AM 1.5, 100 mW/cm^2, the sample was found to generate no photovoltaic effect. Moreover, on a glass-made substrate was formed a p-type semiconductor layer used in Experiment 6, on which in turn was formed a first transparent conductive layer in the same manner as Comparative Experiment 1-1. The initial sheet resistance and the sheet resistance after a time lapse of 1000 hours at a temperature of 120° C. were measured and found to be 69.5 (Ω/□) and 83.2 (Ω/□) respectively.

[0105] (Comparative Experiment 6-2)

[0106] Next, the second transparent conductive layer was checked for its single-film characteristics. As in Experiment 6, on a Mo/glass-made substrate was formed a p-type semiconductor layer comprised of $CuInSe_2$, on which in turn was formed a second transparent conductor layer with a film-thickness of 60 nm in the same manner as in Comparative Experiment 1-2, on which in turn was formed cross-shaped collecting electrodes. When its voltage-current characteristic under the dark conditions was checked, the sample was found to be of rectification. When its voltage-current characteristic was checked after light irradiation of AM 1.5, 100 mW/cm^2, the sample was found to have a little photovoltaic effect. Then, on a glass-made substrate was formed a p-type semiconductor layer used in Experiment 6, on which a second transparent conductive layer in the same manner as in Comparative Experiment 1-2. The initial sheet resistance and the sheet resistance after a time lapse of 1000 hours at a temperature of 120° C. were measured and found to be 41.8 (Ω/□) and 43.9 (Ω/□).

[0107] Although p-type microcrystalline silicon (μc-Si:H:B) and polycrystalline $CuInSe_2$ were used as p-type semiconductor layers above, the effects by the present invention are not restricted to the above-mentioned cases and can be obtained as long as semiconductors that have a p-type conductivity are employed.

EXAMPLES

[0108] The effects by the present invention are detailed below with reference to examples, but not restricted to them.

Example 1

[0109] A non-monocrystalline silicon-made solar cell was prepared that has p-type microcrystalline silicon as p-type semiconductor layers and one pin junction as photovoltaic layers. As a support structure, a stainless-steel plate (SUS430BA) with a dimension of 50×50×0.15 (mm) was used, and the DC magnetron sputtering method was used to form reflecting layers comprised of Ag and lower transparent conductive layers comprised of ZnO. These lower transparent conductive layers comprised of ZnO had unevenness in the surface with an average center-line roughness Ra of 0.12 (μm). The RF plasma-enhanced CVD method with a frequency of 13.56 MHz was used to form n-type semiconductor layers comprised of a-Si:H:P, while the VHF plasma-enhanced CVD method with a frequency of 13.56 MHz was used to form p-type semiconductor layers comprised of μc-Si:H:B. Next, like in Experiment 1, a mask was used that has 25 openings with a 6-mm diameter was used to form a first transparent conductive layer and a second transparent conductive layer, then a cross-shaped mask was used to form collecting electrodes. The detailed forming conditions are listed in Table 8. Such solar cells were prepared as many as four. Those solar cells are to be called here **1**A, **1**B, **1**C, and **1**D.

[0110] The solar cell characteristics of those four solar cells are measured under light irradiation of AM 1.5, 100 mW/cm^2. The average conversion efficiency of 4×25 subcells was 7.01 (%).

[0111] Next, thermal tests were conducted on the solar cells. Like in Experiment 1, a solar cell **1**B was placed in a high-temperature environmental testing machine held at a temperature of 120° C. and was measured for its solar cell characteristics after a time lapse of 1000 hours and found to have a conversion efficiency of 6.99 (%)

[0112] Next, light irradiation tests were conducted on the solar cells. The above-mentioned light was continuously applied to a solar cell **1**C held at a temperature of 50° C. and was measured for its solar cell characteristics after a time lapse of 1000 hours and found to have a conversion efficiency of 6.93 (%).

[0113] Next, torsion tests were conducted. In a state where it is fixed at its three corners, a solar cell **1**D was distorted upward by as much as 9.0 (mm) and then downward by the same displacement, which is 6 times the following displacement set forth in the Solar Cell JIS C8917:

$$h=0.021\times(0.05^2+0.05^2)^{0.5}=0.0015\ (m)=1.5\ (mm)$$

[0114] This operation was repeated 100 times and then also to the other three corners in the same manner. No changes were to be observed in the outer appearances and, the conversion efficiency was found to be 6.97 (%) when the solar cell characteristics were measured. The solar cell characteristics of this solar cell including the others are summarized in Table 9. As can be seen from this table, the photovoltaic element according to the present invention was found to be excellent in all of the initial average characteristics (initial characteristics), average characteristics after thermal test (post-thermal-test characteristics), average characteristics after light irradiation (post-light-irradiation characteristics), and average characteristics after torsion test (post-torsion-test characteristics).

Comparative Example 1-1

[0115] Almost the same solar cells as those in Experiment 1 were prepared and similar tests were conducted except that

a single layer of the first transparent conductive layer with a thickness of 60 (nm) was used as a transparent conductive layer like in Comparative Experiment 1-1. The results are summarized in Table 9. The results have shown that as compared to those prepared in Example 1, the solar cells of Comparative Example 1-1 are similarly excellent in terms of the initial solar cell characteristics but inferior in terms of thermal tests, light irradiation tests, and torsion tests. After the torsion tests, no changes were to be observed in the outer appearances, but short-circuiting was observed at some sub-cells.

Comparative Example 1-2

[0116] Almost the same solar cells as in Example 1 were prepared and similar tests were conducted except that a single layer of the second transparent conductive layer with a film-thickness of 60 (nm) was used as the transparent conductive layer like in Comparative Experiment 1-2. The results are listed in Table 9. The results have shown that the solar cells used in Comparative Example 1-2 are inferior in terms of the initial solar cell characteristics and in torsion tests. After the torsion tests, no changes were to be observed in the outer appearances but short-circuiting was observed at some sub-cells.

[0117] As can be seen from the above description, the photovoltaic element according to the present invention was found to be superior to the conventional photovoltaic elements in all of the initial characteristics, post-thermal-test characteristics, post-light-irradiation characteristics, and post-torsion-test characteristics.

Example 2

[0118] In this example, non-monocrystalline silicon solar cells having a configuration shown in **FIG. 15** were prepared that have p-type microcrystalline silicon carbide (μc-SiC:H:B) as p-type semiconductor layers and one pin junction as photovoltaic layers. A support structure was comprised of glass with a dimension of 100×10×1.0 (mm), and like in Example 1, a second transparent conductive layer and a first transparent conductive layer were stacked sequentially except that the second transparent conductive later had a tin oxide content of 15 mole %. Next, on the first transparent conductive layer was formed a p-type semiconductor layer, by the microwave plasma-enhanced CVD method, which is comprised of microcrystalline silicon carbide, on which were also formed an i-type semiconductor layer and an n-type semiconductor layer like in Example 1. Next, the DC magnetron sputtering method was used to sequentially stack a lower transparent conductive layer comprised of ZnO and a reflecting layer comprised of Ag. This lower transparent conductive layer comprised of ZnO had unevenness in its surface and an average center-line roughness Ra of 0.10 (μm). Such solar cells were prepared as many as four. Those solar cells are to be called **2**A, **2**B, **2**C, and **2**D. The detailed forming conditions are listed in Table 10.

[0119] Those four solar cells were measured for their solar cell characteristics under a light irradiation of AM 1.5, 100 mW/cm^2. The average conversion efficiency of these four solar cells was found to be 7.25 (%).

[0120] Next, like in Example 1, thermal tests were conducted on those solar cells, after which the conversion efficiency of a solar cell **2**B was 7.24 (%).

[0121] Next, light irradiation tests were conducted on those solar cells. After the tests, the conversion efficiency of a solar cell **2**C was 7.17 (%).

[0122] Next, hailing tests were conducted. Under the conditions with a hail-ball diameter of 25 (mm) and a final speed of 23 (m/sec) taken from the Solar Cell JIS C8917, a total of 100 balls struck the glass surface evenly. Then, the solar cell characteristics were measured, to find the conversion efficiency to be 7.19 (%). This item and the other solar cell characteristics are listed in Table 11. As can be seen from this table, the photovoltaic element according to the present invention is superior in all of the initial characteristics, the post-thermal-test characteristics, the post-light-irradiation characteristics, and the post-torsion-test characteristics.

[0123] (Experiment 2-1)

[0124] Almost the same solar cells as those in Example 2 were prepared and similar tests were conducted except that a single layer of a fist transparent conductive layer with a film-thickness of 60 (nm) was used as the transparent conductive layer likely in Comparative Example 1-1. The results are indicated in Table 11. The results have shown that the solar cells of Comparative Example 2-1 are excellent in the initial solar cell characteristics like those in Example 2 but inferior to them in the thermal test, the light irradiation test, and the hailing test. Also, the surface was observed after the hailing test and found to have small peeling with a diameter of 5 pm or so at a few positions. The XMA analysis found that those delaminations occurred at the interface between the transparent conductive layer and the p-type semiconductor layer.

Comparative Example 2-2

[0125] Almost the same solar cells as those in Example 2 were prepared and similar tests were conducted except that a single layer of a second transparent conductive layer was used as the transparent conductive layer like in Comparative Example 1-2. The results are indicated in Table 11. The results have shown that the solar cells in Comparative Example 2-2 are inferior in terms of the initial solar cell characteristics and also in the hailing test. Also, the surface was observed after the hailing test to have small delaminations with a diameter of 10 μm or so at a few positions. The XMA analysis has shown that those delaminations occurred at the interface between the transparent conductive layer and the p-type semiconductor layer.

[0126] As can be seen from the above description, the photovoltaic element according to the present invention is superior to the conventional photovoltaic elements in all of the initial characteristics, the post-thermal-test characteristics, the post-light-irradiation-test characteristics, and the post-torsion-test characteristics.

Example 3

[0127] In this example, solar cells were prepared that employs transparent conductive layers in which the tin concentration changes linearly in the film-thickness direction. Almost the same solar cells were prepared as many as four shown in **FIG. 12** as those in Example 1, except that the transparent conductive layer in Example 1 was made to have such a tin-concentration distribution as shown in **FIG. 4**. In

this example, the target came in indium oxide and tin oxide and the tin oxide target power was changed as time passes so as to provide C_{41}=5 (mole %) and C_{42}=10 (mole %). On these solar cells, almost the same measurement and evaluation as Example 1 were conducted and came up with a result that the solar cells in Example 3 are a little superior to those in Example 1 in all of the four items of characteristics, i.e. open-circuit voltage, short-circuit current, fill factor, and conversion efficiency. Those solar cells were also found to have almost the same change rate in the thermal test but, in the light irradiation test and the torsion test, to have a better change rate than those in Example 1.

Example 4

[0128] In this example, such solar cells were prepared as many as four that uses transparent conductive layers shown in **FIG. 5** in which the tin concentration steeply changes near the p-type semiconductor layer. They were so prepared so as to provide C_{51}=1 (mole %) and C_{52}=15 (mole %) in **FIG. 5**. Here, as the target, the indium oxide and tin oxide were provided and argon and oxygen were used as a sputtering gas, so that the tin target power was changed as time passes. Almost the same measurement and evaluation as Example 1 were conducted on those solar cells and found that they are a little superior to those solar cells in Example 1 in all of the four items of characteristics, i.e. open-circuit voltage, short-circuit current, fill factor, and conversion efficiency. Also, the change rate in the thermal test, the light irradiation, and the torsion test was found to be better than those in Example 1.

Example 5

[0129] In this example, such solar cells were prepared as many as four that use a layer configuration shown in **FIG. 2**. They were so prepared as to provide C_{21}=3 (mole %), C_{22}=10 (mole %), and C_{23}=15 (mole %). Also, the fist, second, and third transparent conductive layers had the film thickness of 10 (nm), 10 (nm), and 40 (nm) respectively. Almost the same measurement and evaluation as Example 1 were conducted on those solar cells and found that they are a little superior to those in Example 1 in all four items of characteristics, i.e. open-circuit voltage, short-circuit current, fill factor, and conversion efficiency. Also, they were found to have a better change rate in the thermal test, the light irradiation test, and the torsion test than those in Example 1.

Example 6

[0130] In this example, four solar cells were prepared that have a pinpin junction with such a configuration as shown in **FIG. 13**. As the second i-type semiconductor layer, a-Si:H was used that is formed by the RF plasma-enhanced CVD method with a frequency of 13.56 MHz. The forming conditions for each layer are indicated in Table 12. Also, almost the same tests as those in Example 1 were conducted to measure the solar cell characteristics. The results are indicated in Table 13. As can be seen from this table, the photovoltaic element according to the present invention is superior to the conventional ones in all of the initial characteristics, the post-thermal-test characteristics, the post-light-irradiation characteristics, and the post-torsion-test characteristics.

Comparative Example 6-1

[0131] Almost the same solar cells as those in Example 6 were prepared and similar tests were conducted, except that a single layer of the first transparent conductive layer was used as the transparent conductive layer as in Comparative Example 1-1. The results are indicated in Table 13. As can be seen from it, the solar cells in Comparative Example 6-1 are excellent likely in Example 6 but inferior to them in the thermal test, the light irradiation test, and the torsion test. After the torsion test, no changes were to be observed in the outer appearances but short-circuiting was observed at some sub-cells.

Comparative Example 6-2

[0132] Almost the same solar cells as those in Example 6 were prepared and similar tests were conducted, except that a single layer of the second transparent conductive layer with a diameter of film-thickness of 60 (nm) was used as the transparent conductive layer as in Comparative Example 1-2. The results are indicated in Table 13. As can be seen from it, the solar cells in Comparative Example 6-2 are inferior in terms of the initial solar cell characteristics and also in the torsion test. After the torsion test, no changes were to be observed in the outer appearances but short-circuiting was observed at some sub-cells.

[0133] As mentioned above, the photovoltaic element according to the present invention was found to superior to the conventional photovoltaic elements in all of the initial characteristics, the post-thermal-test characteristics, the post-light-irradiation characteristics, and the post-torsion-test characteristics.

Example 7

[0134] In this example, four solar cells using n-type monocrystalline silicon substrates formed by the CZ method were prepared. First, on one side of the n-type monocrystalline silicon substrate, phosphorous ions were implanted under the conditions of 30 (keV) and 1×10^{15} (particles/cm^2), to form n^+-type semiconductor layers. On the other side also, boron ions were implanted under the conditions of 100 (keV) and 8×10^{15} (particles/cm^2), to form p^+-type semiconductor layers. Next, they underwent annealing for 30 minutes at a temperature of 950 degrees Celsius in an atmosphere of nitrogen. Next, first and second transparent conductive layers having a 6-mm diameter were formed-as ?many as 25 each under the forming conditions indicated in Table 14, to finally form collecting electrodes consisting of cross-shaped Al's similar to those in Example 1. On these four solar cells, almost the same tests as those in Example 2 were conducted. The solar cell characteristics are indicated in Table 15. As can be seen from it, the photovoltaic element according to the present invention is superior in all of the initial characteristics, the post-thermal-test characteristics, the post-light-irradiation characteristics, and the post-hailing-test characteristics. After the hailing test, no changes were to be observed in the outer appearances.

Comparative Example 7-1

[0135] Almost the same solar cells as those in Example 7 were prepared and similar tests were conducted, except that a single layer of a transparent conductive layer with a film-thickness of 70 (nm) was used as the transparent conductive layer was used like in Comparative Example 2-1. The results are indicated in Table 15. The results have shown that the solar cells prepared in Comparative Example 7-1 are excellent in the initial solar cell characteristics likely in Example 7 but inferior to them in the thermal test, the light

irradiation test, and the hailing test. After the hailing test, the surface was observed to have small delaminations having a diameter of 1 μm at a few positions. The XMA analysis has shown that those delaminations occurred at the interface between the transparent conductive layer and the p-type semiconductor layer.

Comparative Example 7-2

[0136] Almost the same solar cells as those in Example 7 were prepared and similar tests were conducted, except that a single layer of a second transparent conductive layer with a film thickness of 70 (nm) was used as the transparent conductive layer likely in Comparative Example 2-2. The results are indicated in Table 15. The results have shown that the solar cells prepared in Comparative Example 7-2 are inferior in terms of the initial solar cell characteristics and also in the torsion test. Also, after the hailing test, the surface was observed to have small delaminations with a diameter of 10 um or so at a few positions. The XMA analysis has shown that those delaminations occurred at the interface between the transparent conductive layer and the p-type semiconductor layer.

[0137] As mentioned above, the photovoltaic element according to the present invention is superior to the conventional photovoltaic elements in all of the initial characteristics, the post-thermal-test characteristics, the post-light-irradiation characteristics, the post-torsion-test characteristics, and the post-hailing-test characteristics.

[0138] According to the present invention, there can be provided a photovoltaic element having a high open circuit voltage, short circuit current and conversion efficiency. Further, it is possible to improve the thermal stability, stability to continuous light irradiation and mechanical strength of a photovoltaic element. In addition, since the resistance of the transparent conductive layer can be made small, it is possible to broaden the distance between the collecting electrodes, so that the module efficiency can be increased.

TABLE 1

(Experiment 1)

	Substrate (stainless steel)									
	Forming method	Main component	Dopant	SiH_4 (sccm)	H_2 (sccm)	BF_3 (sccm)	Power (W)	Pressure (Pa)	Temperature (° C.)	Layer thickness (nm)
P-type semiconductor layer	RE plasma CVD	μc-Si:H	B	1	50	0.1	40	200	180	50

	Forming method	Main component	Dopant	SnO_2 concentration of target (mole %)	Ar (sccm)	He (sccm)	Power (W)	Pressure (Pa)	Temperature (° C.)	Layer thickness (nm)
first transparent conductive layer	DC magnetron sputtering	In_2O_3	SnO_2	5	30	0	200	0.532	200	10
second transparent conductive layer	DC magnetron sputtering	In_2O_3	SnO_2	10	30	0	200	0.532	200	50
Collecting electrode	DC magnetron sputtering	Al	—	—	30	0	500	0.532	30	200

Dark state voltage-current characteristics: ohmic
Photovoltaic effect: none
P-type semiconductor layer and
first and second transparent conductive layers stacked on glass substrate

Initial sheet resistance	Sheet resistance after heat resistance test
(Ω/□)	(Ω/□)
48.0	50.8

[0139]

TABLE 2

(Comparative Experiment 1-1)

	Substrate (stainless steel)									
	Forming method	Main component	Dopant	SiH_4 (sccm)	H_2 (sccm)	BF_3 (sccm)	Power (W)	Pressure (Pa)	Temperature (° C.)	Layer thickness (nm)
P-type semiconductor layer	RF plasma CVD	μc-Si:H	B	1	50	0.1	40	200	180	50

TABLE 2-continued

(Comparative Experiment 1-1)

	Forming method	Main component	Dopant	SnO_2 concentration of target (mole %)	Ar (sccm)	He (sccm)	Power (W)	Pressure (Pa)	Temperature (° C.)	Layer thickness (nm)
first transparent conductive layer	DC magnetron sputtering	In_2O_3	SnO_2	5	30	0	200	0.532	200	60
Collecting electrode	DC magnetron sputtering	Al	—	—	30	0	500	0.532	30	200

Dark state voltage-current characteristics: ohmic
Photovoltaic effect: none
P-type semiconductor layer and
first transparent conductive layer stacked on glass substrate

Initial sheet resistance	Sheet resistance after heat resistance test	Tin concentration
(Ω/□)	(Ω/□)	(mole %)
70.4	85.1	5.1

[0140]

TABLE 3

(Comparative Experiment 1-2)

Substrate (stainless steel)

	Forming method	Main component	Dopant	SiH_4 (sccm)	H_2 (sccm)	BF_3 (sccm)	Power (W)	Pressure (Pa)	Temperature (° C.)	Layer thickness (nm)
P-type semiconductor layer	RF plasma CVD	μc-Si:H	B	1	50	0.1	40	200	180	50

	Forming method	Main component	Dopant	SnO_2 concentration of target (mole %)	Ar (sccm)	He (sccm)	Power (W)	Pressure (Pa)	Temperature (° C.)	Layer thickness (nm)
second transparent conductive layer	DC magnetron sputtering	In_2O_3	SnO_2	10	30	0	200	0.532	200	60
Collecting electrode	DC magnetron sputtering	Al	—	—	30	0	500	0.532	30	200

Dark state voltage-current characteristics: ohmic
Photovoltaic effect: none
P-type semiconductor layer and
second transparent conductive layer stacked on glass substrate

Initial sheet resistance	Sheet resistance after heat resistance test	Tin concentration
(Ω/□)	(Ω/□)	(mole %)
70.4	85.1	5.1

[0141]

TABLE 4

(Experiment 2)

	Substrate (stainless steel)									
	Forming method	Main component	Dopant	SiH_4 (sccm)	H_2 (sccm)	BF_3 (sccm)	Power (W)	Pressure (Pa)	Temperature (° C.)	Layer thickness (nm)
P-type semiconductor layer	RF plasma CVD	μc-Si:H	B	1	50	0.1	40	200	180	50
	Forming method	Main component	Dopant	Weight ratio of (metal Sn)/(metal In)	O_2 (sccm)			Pressure (mPa)	Temperature (° C.)	Layer thickness (nm)
first transparent conductive layer	Resistance heating vacuum evaporation	In_2O_3	SnO_2	1	30			66.5	200	60
	Forming method	Main component	Dopant	SnO_2 concentration of target (mole %)	Ar (sccm)	He (sccm)	Power (W)	Pressure (Pa)	Temperature (° C.)	Layer thickness (nm)
second transparent conductive layer	DC magnetron sputtering	In_2O_3	SnO_2	15	30	0	200	0.532	200	50
Collecting electrode	DC magnetron sputtering	Al	—	—	30	0	500	0.532	30	200

Dark state voltage-current characteristics: ohmic
Photovoltaic effect: none
P-type semiconductor layer and
first and second transparent conductive layers stacked on glass substrate

Initial sheet resistance	Sheet resistance after heat resistance test
(Ω/□)	(Ω/□)
50.3	52.3

[0142]

TABLE 5

(Comparative Experiment 2-1)

	Substrate (stainless steel)									
	Forming method	Main component	Dopant	SiH_4 (sccm)	H_2 (sccm)	BF_3 (sccm)	Power (W)	Pressure (Pa)	Temperature (° C.)	Layer thickness (nm)
P-type semiconductor layer	RE plasma CVD	μc-Si:H	B	1	50	0.1	40	200	180	50
	Forming method	Main component	Dopant	Weight ratio of (metal Sn)/(metal In) (mole %)	O_2 (sccm)			Pressure (Pa)	Temperature (° C.)	Layer thickness (nm)
first transparent conductive layer	Resistance heating vacuum evaporation	In_2O_3	SnO_2	1	30			0.0665	200	60
Collecting electrode	DC magnetron sputtering	Al	—	—	30	0	500	0.532	30	200

TABLE 5-continued

(Comparative Experiment 2-1)

Dark state voltage-current characteristics: ohmic
Photovoltaic effect: none
P-type semiconductor layer and
first transparent conductive layer stacked on glass substrate

Initial sheet resistance	Sheet resistance after heat resistance test	Tin concentration
(Ω/□)	(Ω/□)	(mole %)
205	730	0.9

[0143]

TABLE 6

(Comparative Experiment 2-2)

Substrate (stainless steel)

	Forming method	Main component	Dopant	SiH_4 (sccm)	H_2 (sccm)	BF_3 (sccm)	Power (W)	Pressure (Pa)	Tempe-rature (° C.)	Layer thickness (nm)
P-type semi-conductor layer	RF plasma CVD	μc-Si:H	B	1	50	0.1	40	200	180	50

	Forming method	Main component	Dopant	SnO_2 concentration of target (mole %)	Ar (sccm)	He (sccm)	Power (W)	Pressure (Pa)	Tempe-rature (° C.)	Layer thickness (nm)
second transparent conductive layer	DC magnetron sputtering	In_2O_3	SnO_2	10	30	0	200	0.532	200	60
Collecting electrode	DC magnetron sputtering	Al	—	—	30	0	500	0.532	30	200

Dark state voltage-current characteristics: ohmic
Photovoltaic effect: none
P-type semiconductor layer and
first transparent conductive layer stacked on glass substrate

Initial sheet resistance	Sheet resistance after heat resistance test	Tin concentration
(Ω/□)	(Ω/□)	(mole %)
37.7	38.5	15.5

[0144]

TABLE 7

Experiment 3

Tin concentration (mole %)	Initial sheet resistance (Ω/□)	Sheet resistance after heat resistance test (Ω/□)	Rate of change
1.1	185	320	1.73
2.3	105	156	1.49
5.1	70.4	85.1	1.21
8.5	56.2	61.2	1.09
10.3	42.1	44.3	1.05
12.1	39.5	40.6	1.03
15.5	37.7	38.5	1.02

TABLE 7-continued

Experiment 3

Tin concentration (mole %)	Initial sheet resistance (Ω/□)	Sheet resistance after heat resistance test (Ω/□)	Rate of change
19.5	35.6	36.0	1.01
23.5	41.1	42.0	1.02
26.7	53.0	54.6	1.03
29.2	57.3	59.6	1.04
33.2	60.2	63.2	1.05

[0145]

TABLE 8

(Example 1)

	Substrate (stainless steel)										
	Forming method	Main component	Dopant	Target	Ar (sccm)	He (sccm)		Power (W)	Pressure (Pa)	Tempe-rature (° C.)	Layer thickness (nm)
Reflecting layer	DC magnetron sputtering	Ag		Ag	25			400	0.665	300	800
Lower trans-parent con-ductive layer	DC magnetron sputtering	ZnO		ZnO	25			400	0.665	300	1300
	Forming method	Main component	Dopant	SiH_4 (sccm)	H_2 (sccm)	BF_3 (sccm)	PH_3 (sccm)	Power (W)	Pressure (Pa)	Tempe-rature (° C.)	Layer thickness (nm)
N-type semi-conductor layer	RF Plasma CVD	a-Si:H	P	1	50	0.1	2	172.9	200	10	
I-type semi-conductor layer	VHF plasma CVD	μc-Si:H		100	3000			160	26.6	350	850
P-type semi-conductor layer	RF plasma CVD	μc-Si:H	B	1	=50	0.1		40	200	180	5
	Forming method	Main component	Dopant	SnO_2 concentration of target(mole%)	Ar (sccm)	He (sccm)		Power (W)	Pressure (Pa)	Tempe-rature (° C.)	Layer thickness (nm)
first transparent conductive layer	DC magnetron sputtering	In_2O_3	SnO_2	5	30	0		200	0.532	200	10
second transparent conductive layer	DC magnetron sputtering	In_2O_3	SnO_2	10	30	0		200	0.532	200	50
Collecting electrode	DC magnetron sputtering	Al	—	—	30	0		500	0.532	30	200

[0146]

TABLE 9

	Initial average characteristics				Average characteristics after thermal test			
	Open circuit voltage (V)	Short circuit current density (mA/cm^2)	Fill factor	Conversion efficiency (%)	Open circuit voltage (V)	Short circuit current density (mA/cm^2)	Fill factor	Conversion efficiency (%)
Example 1	0.455	24.5	0.629	7.01	0.454	24.5	0.628	6.99
Rate after test					0.998	1.000	0.998	0.996
Comparative Example 1-1	0.455	24.6	0.625	7.00	0.454	24.4	0.586	6.49
Rate after test					0.998	0.992	0.938	0.928
Comparative Example 1-2	0.432	23.7	0.622	6.37	0.432	23.7	0.622	6.37
Rate after test					1.000	1.000	1.000	1.000

	Average characteristics after light irradiation test				Average characteristics after torsion test			
	Open circuit voltage (V)	Short circuit current density (mA/cm^2)	Fill factor	Conversion efficiency (%)	Open circuit voltage (V)	Short circuit current density (mA/cm^2)	Fill factor	Conversion efficiency (%)
Example 1	0.453	24.4	0.627	6.93	0.453	24.5	0.628	6.97
Rate after test	0.996	0.996	0.997	0.988	0.996	1.000	0.998	0.994
Comparative Example 1-1	0.451	24.4	0.596	6.56	0.442	24.3	0.576	6.19
Rate after test	0.991	0.992	0.954	0.938	0.971	0.988	0.922	0.884

TABLE 9-continued

	Comparative Example 1-2	0.429	23.6	0.619	6.27	0.428	23.7	0.617	6.26
	Rate after test	0.993	0.996	0.995	0.984	0.991	1.000	0.992	0.983

Rate after test = (Characteristics after test)/(Initial characteristics)

[0147]

TABLE 10

(Example 2)

	Substrate (stainless steel)										
	Forming method	Main component	Dopant	SnO_2 concentration of target (mole %)	Ar (sccm)	He (sccm)		Power (W)	Pressure (Pa)	Temperature (° C.)	Layer thickness (nm)
second transparent conductive layer	DC magnetron sputtering	In_2O_3	SnO_2	15	30	0		200	0.532	200	50
first transparent conductive layer	DC magnetron sputtering	In_2O_3	SnO_2	5	30	0		200	0.532	200	10
	Forming method	Main component	Dopant	SiH_4 (sccm)	H_2 (sccm)	BF_3 (sccm)	PH_3 (sccm)	CH_4 (sccm)	Power (W)	Pressure (Pa)	Temperature (° C.)	Layer thickness (nm)
P-type semiconductor layer	MW plasma CVD	μc-SiC:H	B	10	50	0.1		2.5	400	1.33	350	5
I-type semiconductor layer	VHF plasma CVD	μc-Si:H		100	3000				160	26.6	350	850
N-type semiconductor layer	RF plasma CVD	a-Si:H	P	1	50		0.1		2	172.9	200	10
	Forming method	Main component	Dopant	Target	Ar (sccm)				Power (W)	Pressure (Pa)	Temperature (° C.)	Layer thickness (nm)
Lower transparent conductive layer	DC magnetron sputtering	ZnO		ZnO	25				400	0.665	300	1300
Reflecting layer	DC magnetron sputtering	Ag		Ag	25				400	0.665	30	100

[0148]

TABLE 11

	Initial average characteristics				Average characteristics after thermal test			
	Open circuit voltage (V)	Short circuit current density (mA/cm^2)	Fill factor	Conversion efficiency (%)	Open circuit voltage (V)	Short circuit current density (mA/cm^2)	Fill factor	Conversion efficiency (%)
Example 2	0.468	24.8	0.625	7.25	0.467	24.8	0.625	7.24
Rate after test					0.998	1.000	1.000	0.998
Comparative Example 2-1	0.467	24.9	0.623	7.24	0.465	24.7	0.589	6.76
Rate after test					0.996	0.992	0.945	0.934

TABLE 11-continued

Comparative Example 2-2	0.452	24.1	0.620	6.75	0.451	24.0	0.619	6.70
Rate after test					0.998	0.996	0.998	0.992

	Average characteristics after light irradiation test				Average characteristics after torsion test			
	Open circuit voltage (V)	Short circuit current density (mA/cm^2)	Fill factor	Conversion efficiency (%)	Open circuit voltage (V)	Short circuit current density (mA/cm^2)	Fill factor	Conversion efficiency (%)
Example 2	0.467	24.6	0.624	7.17	0.466	24.7	0.625	7.19
Rate after test	0.998	0.992	0.998	0.988	0.996	0.996	1.000	0.992
Comparative Example 2-2	0.465	24.8	0.572	6.60	0.458	24.6	0.612	6.90
Rate after test	0.996	0.996	0.918	0.911	0.981	0.988	0.982	0.952
Comparative Example 1-2	0.450	24.0	0.619	6.69	0.445	24.0	0.617	6.59
Rate after test	0.996	0.996	0.998	0.990	0.985	0.996	0.995	0.976

Rate after test = (Characteristics after test)/(Initial characteristics)

[0149]

TABLE 12

(Example 6)

Substrate (stainless steel)

	Forming method	Main component	Dopant	Target	Ar (sccm)	He (sccm)	Power (W)	Pressure (Pa)	Temperature (° C.)	Layer thickness (nm)
Reflecting layer	DC magnetron sputtering	Ag		Ag	25		400	0.665	300	800
Lower transparent conductive layer	DC magnetron sputtering	ZnO		ZnO	25		400	0.665	300	1300

	Forming method	Main component	Dopant	SiH_4 (sccm)	H_2 (sccm)	BF_3 (sccm)	PH_3 (sccm)	Power (W)	Pressure (Pa)	Temperature (° C.)	Layer thickness (nm)
first n-type semiconductor layer	RE Plasma CVD	a-Si:H	P	1	50		0.1	2	172.9	200	10
first i-type semiconductor layer	VHF plasma CVD	μc-Si:H		100	3000			160	26.6	350	850
first p-type semiconductor layer	RF plasma CVD	μc-Si:H	B	1	50	0.1		40	200	180	5
second n-type semiconductor layer	RF plasma CVD	a-Si:H	P	1	50		0.1	2	172.9	200	10
second i-type semiconductor layer	RF plasma CVD	a-Si:H		2	50			2	172.9	200	350
second p-type semiconductor layer	RF plasma CVD	μc-Si:H	B	1	50	0.1		40	200	180	5

	Forming method	Main component	Dopant	SnO_2 concentration of target (mole %)	Ar (sccm)	He (sccm)	Power (W)	Pressure (Pa)	Temperature (° C.)	Layer thickness (nm)
first transparent conductive layer	DC magnetron sputtering	In_2O_3	SnO_2	3	30	5	200	0.532	180	20
second transparent conductive layer	DC magnetron sputtering	In_2O_3	SnO_2	15	30	5	200	0.532	180	40
Collecting electrode	DC magnetron sputtering	Al	—	—	30	0	500	0.532	30	200

[0150]

TABLE 13

	Initial average characteristics				Average characteristics after thermal test				Average characteristics after light irradiation test				Average characteristics after torsion test			
	Open circuit voltage (V)	Short circuit current density (mA/cm^2)	Fill factor	Conversion efficiency (%)	Open circuit voltage (V)	Short circuit current density (mA/cm^2)	Fill factor	Conversion efficiency (%)	Open circuit voltage (V)	Short circuit current density (mA/cm^2)	Fill factor	Conversion efficiency (%)	Open circuit voltage (V)	Short circuit current density (mA/cm^2)	Fill factor	Conversion eficiency (%)
Example 6	1.396	13.0	0.712	12.9	1.396	13.0	0.711	12.9	1.382	12.9	0.674	12.0	1.395	13.0	0.710	12.9
Rate after test					1.000	1.000	0.999	0.999	0.990	0.992	0.947	0.930	0.999	1.000	0.997	0.996
Comparative Example 6-1	1.397	13.0	0.709	12.9	1.396	12.9	0.687	12.4	1.381	12.8	0.649	11.5	1.376	12.9	0.695	12.3
Rate after test					0.999	0.992	0.969	0.961	0.989	0.985	0.915	0.891	0.985	0.992	0.980	0.958
Comparative Example 6-2	1.372	12.7	0.712	12.4	1.371	12.7	0.711	12.4	1.360	12.6	0.672	11.5	1.361	12.7	0.692	12.0
Rate after test					0.999	1.000	0.999	0.998	0.991	0.992	0.944	0.928	0.992	1.000	0.972	0.964

Rate after test = (Characteristics after test)/(Initial characteristics)

[0151]

TABLE 14

(Example 7)

	Substrate (stainless steel)				
	Forming method	Main component	Dopant	Temperature (° C.)	Layer thickness (nm)
N^+-type semi-conductor layer	Ion implantation	CZ-Si	P	25	500
N^--type semi-conductor layer		CZ-Si	P		
P^+-type semi-conductor layer	Ion implantation	CZ-Si	B	25	300

	Heat treatment in N_2 atmosphere									
Annealing treatment	Forming Method	Main component	Dopant	SnO_2 concentration of target (mole %)	Ar (sccm)	He (sccm)	Power (W)	Pressure (Pa)	950 Temperature (° C.)	Layer thickness (nm)
first transparent conductive layer	DC magnetron sputtering	In_2O_3	SnO_2	3	30	10	200	0.532	300	20
second transparent conductive layer	DC magnetron sputtering	In_2O_3	SnO_2	15	30	10	200	0.532	300	50
Collecting electrode	DC magnetron sputtering	Al	—	—	30	0	500	0.532	30	200

[0152]

TABLE 15

	Initial average characteristics				Average characteristics after thermal test				Average characteristics after light irradiation test				Average characteristics after hailing test			
	Open circuit voltage (V)	Short circuit current density (mA/cm^2)	Fill factor	Conversion efficiency (%)	Open circuit voltage (V)	Short circuit current density (mA/cm^2)	Fill factor	Conversion efficiency (%)	Open circuit voltage (V)	Short circuit current density (mA/cm^2)	Fill factor	Conversion efficiency (%)	Open circuit voltage (V)	Short circuit current density (mA/cm^2)	Fill factor	Conversion efficiency (%)
Example 7	0.604	29.2	0.771	13.6	0.604	29.2	0.771	13.6	0.604	29.2	0.771	13.6	0.601	29.2	0.768	13.5
Rate after test					1.000	1.000	1.000	1.000	1.000	1.000	1.000	1.000	0.995	1.000	0.996	0.991

TABLE 15-continued

	Initial average characteristics				Average characteristics after thermal test				Average characteristics after light irradiation test				Average characteristics after hailing test			
	Open circuit voltage (V)	Short circuit current density (mA/cm^2)	Fill factor	Conversion efficiency (%)	Open circuit voltage (V)	Short circuit current density (mA/cm^2)	Fill factor	Conversion efficiency (%)	Open circuit voltage (V)	Short circuit current density (mA/cm^2)	Fill factor	Conversion efficiency (%)	Open circuit voltage (V)	Short circuit current density (mA/cm^2)	Fill factor	Conversion efficiency (%)
Comparative Example 7-1	0.604	29.3	0.771	13.6	0.604	29.2	0.758	13.4	0.604	29.3	0.760	13.4	0.597	29.2	0.721	12.6
Rate after test					1.000	0.997	0.983	0.980	1.000	1.000	0.986	0.986	0.988	0.997	0.935	0.921
Comparative Example 7-2	0.591	28.3	0.772	12.9	0.591	28.3	0.757	12.7	0.591	28.3	0.767	12.8	0.581	28.3	0.754	12.4
Rate after test					1.000	1.000	0.981	0.981	1.000	1.000	0.994	0.994	0.983	1.000	0.977	0.960

Rate after test = (Characteristics after test)/(Initial characteristics)

What is claimed is:

1. A photovoltaic element comprising a p-type semiconductor layer and a transparent conductive layer comprised of indium tin oxide bonded to each other at a surface, wherein the transparent conductive layer comprises a plurality of layers, and wherein the sum of tin oxide content and tin content of a layer of the plurality of layers closest to the bonding surface of the p-type semiconductor layer and the transparent conductive layer is less than the sum of tin oxide content and tin content of any of the other layers.

2. The photovoltaic element according to claim 1, wherein the sum of tin oxide content and tin content of the layer closest to the bonding surface is not more than 10 mole %.

3. The photovoltaic element according to claim 1, wherein a layer having the maximum of the sum of tin oxide content and tin content of the other layers of the plurality of layers has the sum of tin oxide content and tin content of not less than 12 mole % and not more than 30 mole %.

4. The photovoltaic element according to claim 1, wherein the thickness of the layer closest to the bonding surface is not more than a half of the whole thickness of the transparent conductive layer.

5. The photovoltaic element according to claim 1, wherein the thickness of a layer having the maximum of the sum of tin oxide content and tin content of the other layers of the plurality of layers is not less than a half of the whole thickness of the transparent conductive layer.

6. A photovoltaic element comprising a p-type semiconductor layer and a transparent conductive layer comprised of indium tin oxide bonded to each other at a surface, wherein the sum of tin oxide content and tin content of the transparent conductive layer varies successively in the layer thickness direction and is minimum at the bonding surface of the p-type semiconductor layer and the transparent conductive layer.

7. The photovoltaic element according to claim 6, wherein the sum of tin oxide content and tin content of the transparent conductive layer at the bonding surface is not more than 10 mole %.

8. The photovoltaic element according to claim 6, wherein a region having the maximum of the sum of tin oxide content and tin content of the transparent conductive layer has the sum of tin oxide content and tin content of not less than 12 mole % and not more than 30 mole %.

9. The photovoltaic element according to claim 6, wherein the thickness of a region having the sum of tin oxide content and tin content of not more than 10 mole % of the transparent conductive layer is not more than a half of the whole thickness of the transparent conductive layer.

10. The photovoltaic element according to claim 6, wherein the thickness of a region having the sum of tin oxide content and tin content of not less than 12 mole % of the transparent conductive layer is not less than a half of the whole thickness of the transparent conductive layer.

11. A photovoltaic element comprising a p-type semiconductor layer and a transparent conductive layer comprised of indium tin oxide bonded to each other at a surface in a thermal equilibrium state, wherein the lower edge energy of the conduction band of the transparent conductive layer varies in the layer thickness direction, and wherein the difference between the lower edge energy of the conduction band of the transparent conductive layer and the Fermi level in the vicinity of the bonding surface of the p-type semiconductor layer and the transparent conductive layer is larger than an average of the difference therebetween of the whole of the transparent conductive layer.

* * * * *